

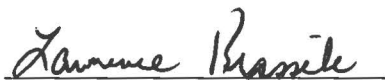
Record of Late Pleistocene Ice Rafted Debris at IODP Site 1308 in the Central North Atlantic

Senior Research Thesis
Submitted as Partial Fulfillment of the Graduation Requirements
For the Bachelors Degree in Geological Sciences
At The Ohio State University

By
Katherine E. Bechtel

The Ohio State University
2015

Approved by:



Dr. Lawrence A. Krissek
School of Earth Sciences

TABLE OF CONTENTS

Abstract	ii
Acknowledgments	iii
List of Tables	iv
List of Figures	v
Introduction	1
Goals and Objectives	2
Literature Review	3
Methods	5
Results	8
Discussion	20
Conclusions	36
Recommendations Regarding Future Research	36
References Cited	38
Appendix	39

Abstract

Ice rafted debris (IRD) consists of rock grains of terrestrial origin that were transported by glacial icebergs. These grains may provide clues to past climate, ocean currents and other geologic conditions. Samples from the North Atlantic Integrated Ocean Drilling Program (IODP) Site 1308 have been examined to collect information on IRD abundances downcore. In this study a total of 39 samples have been inspected and range in age from 851.5 to 969.625 kya. These data were compared to known glacial stage data in order to see if the abundance of ice rafted debris corresponds to global climate state through time.

The abundances of specific grain types were acquired through a census of 100 grains from each sample, which were taken at a spacing of 10 to 30 cm in the core. The terrestrial grains showed fluctuations in abundances within the core. Terrestrial abundances increased near the boundaries of the glacial/interglacial stages for both the individual grain categories and the terrestrial group as a whole. Some IRD grain types are site-specific, allowing the determination of iceberg provenance. The grains were found to originate from Canada, Iceland/central East Greenland, and southern Greenland.

Acknowledgements

First off I would like to thank Dr. Larry Krissek for providing me the opportunity to be part of this continuing research project and the guidance he provided throughout my experience.

Thanks to all previous students that contributed to this research project in the past especially Colin Whyte.

I would also like thank the Integrated Ocean Drilling Program that obtained the cores and the Bremen Core Repository for providing the samples for undergraduate research.

Thank you to all my professors, teachers, friends, and family for everything you have done for me.

Finally, a special thanks to my parents. Thank you for all of the patience, knowledge, and support you have given me over the years.

List of Tables:

Table 1: Variation in Sample Recount	7
Table 2: Variation in Sample recount – individual grain types	8
Table 3: MIS Stage and Age	17

List of Figures:

Figure 1: Site 1308 Map	4
Figure 2: Total Terrestrial Grains vs. Depth	9
Figure 3: Total Biological Grains vs. Depth	10
Figure 4: Total Other Grains vs. Depth	11
Figure 5: Total Quartz Grains vs. Depth	12
Figure 6: Total Coarse Grained Mafic Grains vs. Depth	13
Figure 7: Total Fine Grained Mafic Grains vs. Depth	14
Figure 8: Total Volcanic Grains vs. Depth	15
Figure 9: Total Sedimentary and Carbonate Fragments vs. Depth.....	16
Figure 10: Total Terrestrial Grains vs. Age with MIS Stages	18
Figure 11: Total Biological Grains vs. Age with MIS Stages	19
Figure 12: Total Other Grains vs. Age with MIS Stages	20
Figure 13: Total Coarse Grained Mafic Grains vs. Age with MIS Stages	21
Figure 14: Total Quartz Grains vs. Age with MIS Stages	22
Figure 15: Total Fine Grained Mafic Grains vs. Age with MIS Stages	23
Figure 16: Total Volcanic Grains vs. Age with MIS Stages	24
Figure 17: Total Sedimentary and Carbonate Fragments vs. Age with MIS Stages.....	25
Figure 18: Total Terrestrial Grains Mudball-free	28
Figure 19: Total Biological Grains Mudball-free	29
Figure 20: Total Coarse Grained Mafic Grains Mudball-free	30
Figure 21: Total Quartz Grains vs. Mudball-free	31
Figure 22: Total Fine Grained Mafic Grains Mudball-free	32
Figure 23: Total Volcanic Grains Mudball-free	33
Figure 24: Total Sedimentary & Carbonate Fragments Mudball-free .	34
Figure 25: Total Terrestrial Mudball-free	35

Introduction

By studying small rock grains from the ocean floor, scientists can reconstruct past climates and glacial behavior. In a glacial region, the ice flows across the landscape, breaking off and picking up rock fragments (Alley et al., 1997). These pieces become trapped within the ice and travel with it as it moves. When the rock fragments reach the glacial terminus, they will be released from the ice and form any of a variety of deposits if on land. If the glacial terminus is at a coastline, though, ice can calve off from the glacier to form icebergs (Dowdeswell and Dowdeswell, 1989). These icebergs carry the land-based grains that are entrained in the ice. These grains are then released as the iceberg melts in the ocean hence becoming ice-rafted debris (IRD) on the seafloor. Geologists can later find and study these grains. Using their relative abundances in relation to the known age of the sediment in which the IRD occurs, scientists can identify glacial changes through time on an individual or global scale, interpret past climate, and determine paleocurrent patterns in past oceans.

This study examines grains in samples taken from Integrated Ocean Drilling Program (IODP) Site 1308 in the North Atlantic. A census was made of grain type and relative abundance within a representative sub sample of 100 grains from each sample. These data were placed into a time framework using age data from a previous study, and the abundances of terrestrial grains, biogenic grains, other grains, and individual grain types were plotted against time. The data were also examined relative to glacial/interglacial marine

isotope stages, in order to identify how strongly the IRD record was controlled by global climate state. IRD provenance was also determined based on grain compositions.

Goals and Objectives

The scientific goal for this research project was to determine the history and source of ice-rafting in the North Atlantic. This was achieved by interpreting the relative abundances of ice-rafted debris overall and the corresponding grain abundances of specific grain lithologies. Individual grain lithologies were analyzed to determine the provenance of the ice-rafted debris. The study had the following objectives:

1. Conduct a grain census to determine the abundance of ice-rafted debris in each sample, and to develop a history of ice-rafting at Site 1308. This history was then compared to the globally defined glacial and interglacial record, in order to examine the relationship between the importance of ice-rafting at Site 1308 and global climate state.
2. Establish IRD provenance by determining the lithologies of the terrigenous grains and linking those lithologies to the geology of nearby localities including Canada, Greenland, and Iceland. Variations in grain abundances of individual lithologies were then used to define glacial fluctuations in these source regions.

Literature Review

Site 1308 is located in the North Atlantic at 49°53'N, 24°14'W with a water depth of 3900m (De Schepper et al., 2009). See map (Figure 1) for site location (Hodell et al., 2008). This location lies within the North Atlantic current which provides a northeastern/southwestern pathway, bridging the cold to mild temperate climate zones of the Atlantic (De Schepper et al., 2009).

The glacial/interglacial history of the North Atlantic has been reconstructed using a variety of proxies, including ice-rafted debris. It has been shown that the preferred method of IRD transport is by icebergs (Krissek and St. John, 2002), rather than. Site 1308 was chosen because it is in deep water, where low energy conditions exist that are unlikely to disturb deposited material, along with a high sedimentation rate. These conditions enhance the likelihood that a more continuous IRD record will be preserved.

The provenance of IRD in the North Atlantic has been researched thoroughly in previous studies. For example, Heinrich events have been interpreted as massive ice rafted debris deposits as a result of sudden collapse of the Laurentide Ice Sheet (Hodell et al., 2008). Within North Atlantic IRD, sedimentary and carbonate grains are interpreted as originating from Canada/Hudson Strait (Hodell et al., 2008); mafic grains originated from Iceland or central East Greenland (Krissek & St. John 2004); and quartz grains originated from southern Greenland or Canada (Krissek & St. John, 2004). With this information, abundances of specific grain types can provide insight into the relative rates at which ice rafted debris was being supplied from the

various sources. This provides information on local glacial behavior for each source area.

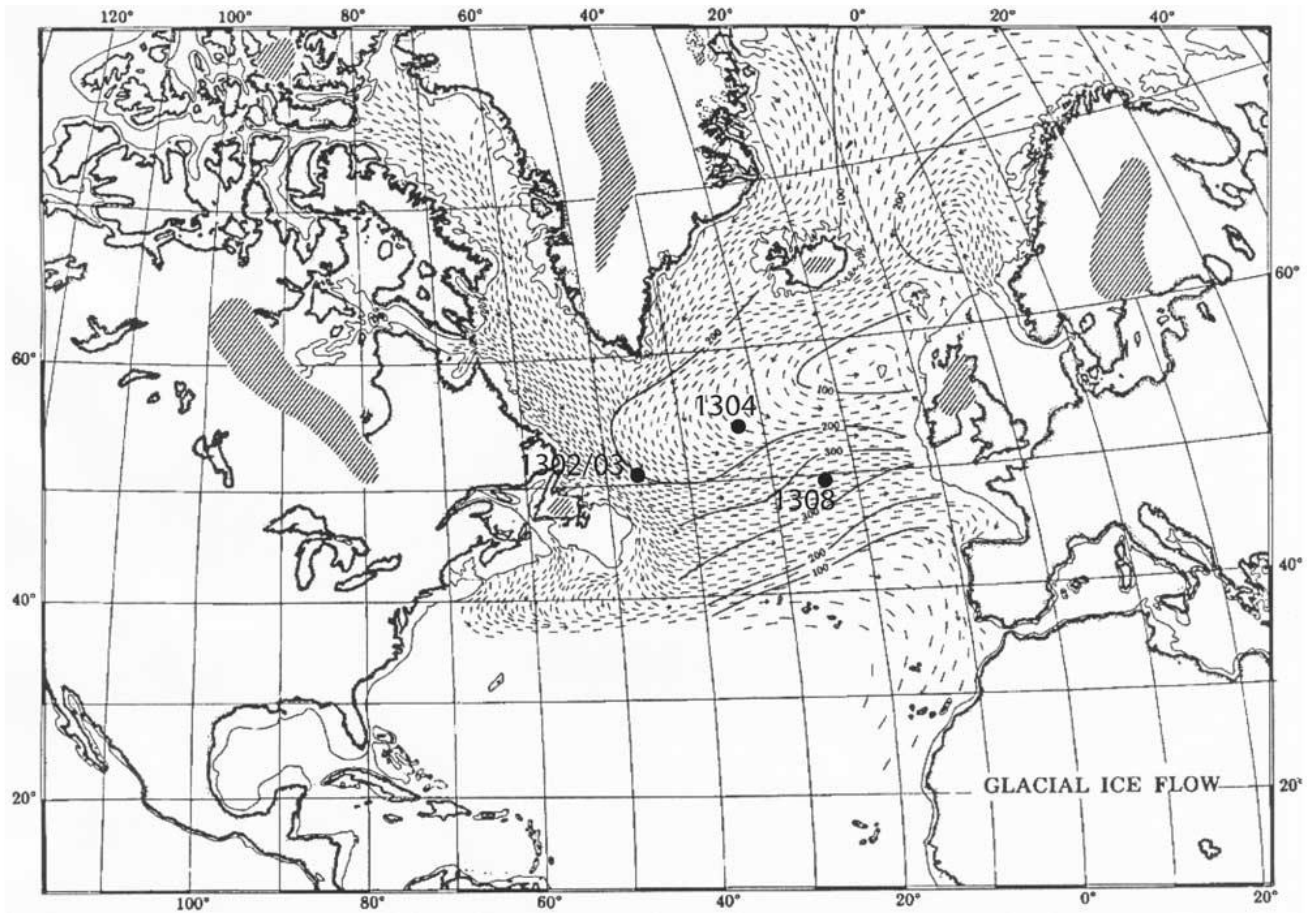


Figure 1: Position of IODP Sites U1302/03, U1304, and U1308 relative to IRD accumulation for the last glaciation (modified after Ruddiman [1977]). Arrows represent mean paths of distribution of ice-rafted debris during glacial periods inferred by Ruddiman (Hodell 2008)

Methods

The samples used for this study were collected from the North Atlantic Site 1308 during Expedition 303 by the Integrated Ocean Drilling Program. In order to obtain a complete stratigraphic section, multiple holes were drilled at Site 1308 and cores were correlated to create a composite core section. Sample depths in this composite core are given in meters composite depth (mcd). The sample depth ranged from 55.58 mcd to 65.03 mcd. Samples were taken every 10–30 cm through the interval studied.

The sample was sieved into three size categories, $>2\text{mm}$, $>150\mu\text{m}$, $<150\mu\text{m}$, preceding this research. That sieving process was as follows:

1. the sample was weighed
2. the sample was oven dried at 40°C for 24 hours
3. the sample was reweighed
4. the sample was placed in an ultrasonic bath for 10 minutes
5. the sample was wet-sieved at 2mm and $150\mu\text{m}$
6. the size separates were dried at 40°C for 24 hours
7. the size separates were weighed
8. the size separates were stored in a labeled glass vials and the weight percent of the $>150\mu\text{m}$ fraction was calculated using the initial dry weight of the entire sample and the dry weight of the $150\mu\text{m}$ – 2mm fraction

The $>150\mu\text{m}$ – 2mm sample fractions of the 39 samples were examined for this study. This size fraction was selected because sand grains were more likely

to have been transported to the offshore location of Site 1308 by ice-rafting than by oceanic currents. A subsample of each sample was examined with a binocular microscope, and a representative field of view was chosen for point-counting. A census of 100 grains was made, with the grain type recorded for each grain. The grain types identified were: mudballs, forams/biological, quartz, coarse grained mafic, fine grained mafic, volcanic, iron stained quartz, rose quartz, pyritic, and sedimentary/carbonate fragments. Mudballs were defined as an aggregation of mud and other small grains that failed to disaggregate during the initial sample processing and sieving. The individual grain types were then combined into three general categories for data representation. Those categories are: Terrestrial (quartz, coarse grained mafic, fine grained mafic, volcanic, iron stained quartz, rose quartz, and sedimentary/carbonate fragments), Biological (forams/biological), and Other (mudballs and pyritic).

Age was calculated for each sample using the sedimentation rate and age data from Hodell et al. (2008). The calculations are thus:

$$1. \text{ Sedimentation rate: } \frac{(65.71-52.58)mcd}{978-814 ky} = 8 \text{ cm/ky}$$

$$2. \text{ Age for each sample: } \frac{[(\text{Sample depth}-52.58)*100]}{8cm/ky} + 814 = \text{sample age}$$

To assess the data reproducibility of this research, 8 randomly selected samples were recounted. The analytical uncertainty of the grain abundance data was then calculated. The method used is as follows:

1. calculate the average of the original and replicate abundances for the sample
2. calculate the difference between the original census counts and the average
3. divide the difference by the average to find the percent uncertainty
4. repeat this process for each sample, and calculate the average of the eight uncertainties for grain type

The average analytical uncertainty ranged from approximately 15% to 6% depending on grain type with the Total average uncertainty is approximately 10%, indicating good precision in the census data (Table 1).

Variation in Sample Recount

	Sample number	Depth (mcd)	% Terr	% Bio	% Mudballs
Most Similar	303-1308-F6-H5-(56-58)-80003091	59.93	2.4	3.0	2.8
	303-1308-F6-H5-(56-58)-80003091 *	59.93			
	303-1308-B7-H5-(28-30)-50001289	65.03	0.9	3.3	6.0
	303-1308-B7-H5-(28-30)-50001289 *	65.03			
Most Different	303-1308-F6-H4-(6-8)-80002925	57.93	0.0	1.7	4.9
	303-1308-F6-H4-(6-8)-80002925 *	57.93			
	303-1308-C6-H5-(56-58)-60003147	55.58	8.8	3.0	18.7
	303-1308-C6-H5-(56-58)-60003147 *	55.58			
	303-1308-C6-H5-(106-108)-60003149	56.08	26.4	21.3	1.4
	303-1308-C6-H5-(106-108)-60003149 *	56.08			
	303-1308-F6-H4-(128-130)-80002930	59.15	10.8	29.8	3.0
	303-1308-F6-H4-(128-130)-80002930 *	59.15			
	303-1308-B7-H5-(6-8)-50001288	64.81	55.9	5.8	5.0
	303-1308-B7-H5-(6-8)-50001288 *	64.81			
	303-1308-B7-H3-(128-130)-50001000	63.03	13.6	4.5	7.1
	303-1308-B7-H3-(128-130)-50001000 *	63.03			
		Average for all the samples of that same type	14.8	9.0	6.1
		Total Average Variation for all Samples	10.0		

Table 1: Total percentages divided into most similar and most different results of the recounted samples

* signifies sample recount

Table 2 shows the uncertainties in the abundances of individual grain types. As might be expected with the generally low number of grains in each category, the analytical uncertainty is higher, averaging approximately 25%. The census still had moderately good precision considering the limited sample sizes and the small abundances of these grains within the samples.

Variation in Sample Recount by Grain type												
	Sample number	Depth (mcd)	% Mudballs	% Forams / Bio	% Quartz	% Coarse Grained Mafic	% Fine grained mafic	% Volcanic	% Iron Stained Quartz	% Rose quartz	% Pyritic	% Sed/ Carb. Fragments
Most Similar	303-1308-F6-H4-(6-8)-80002925	57.93	8.0	1.7	0.0	0.0	0.0	0.0	0.0	0.0	75.4	0.0
	303-1308-F6-H4-(6-8)-80002925 *	57.93										
	303-1308-F6-H4-(128-130)-80002930	59.15	18.7	29.8	13.9	10.5	35.0	7.7	35.0	0.0	0.0	6.3
	303-1308-F6-H4-(128-130)-80002930	59.15										
	303-1308-B7-H3-(128-130)-50001000	63.03	2.9	4.5	1.4	16.3	100.0	51.0	0.0	0.0	0.0	41.7
Most Different	303-1308-B7-H3-(128-130)-50001000	63.03										
	303-1308-C6-H5-(106-108)-60003149	56.08	6.0	21.2	43.5	27.0	100.0	0.0	52.4	0.0	0.0	50.0
	303-1308-C6-H5-(106-108)-60003149	56.08										
	303-1308-C6-H5-(56-58)-60003147	55.58	2.8	3.0	43.3	45.5	100.0	65.9	100.0	0.0	0.0	34.5
	303-1308-C6-H5-(56-58)-60003147 *	55.58										
	303-1308-B7-H5-(6-8)-50001288	64.81	5.0	5.8	30.7	100.0	100.0	0.0	0.0	100.0	0.0	47.8
	303-1308-B7-H5-(6-8)-50001288 *	64.81										
	303-1308-F6-H5-(56-58)-80003091	59.93	1.4	5.8	2.9	47.8	100.0	43.5	0.0	0.0	0.0	100.0
	303-1308-F6-H5-(56-58)-80003091 *	59.93										
	303-1308-B7-H5-(28-30)-50001289	65.03	7.0	3.3	30.3	36.3	34.6	32.5	0.0	100.0	0.0	6.7
	303-1308-B7-H5-(28-30)-50001289 *	65.03										
	Average for all the samples of that type		6.5	9.4	20.8	35.4	71.2	25.1	23.4	25.0	9.4	35.9
	Total Average Variation for all Samples		26.2									

Table 2 : Grain Type percentages divided into most similar and most different results of the recounted samples

* signifies sample recount

Results

Thirty-nine samples were analyzed, with the sample at a depth of 56.43 mcd and an age of 862.125 kya missing. The grain percentage data are summarized in Appendix A. The census data revealed varying grain abundances throughout the section studied, as seen in Figures 2–9. Some

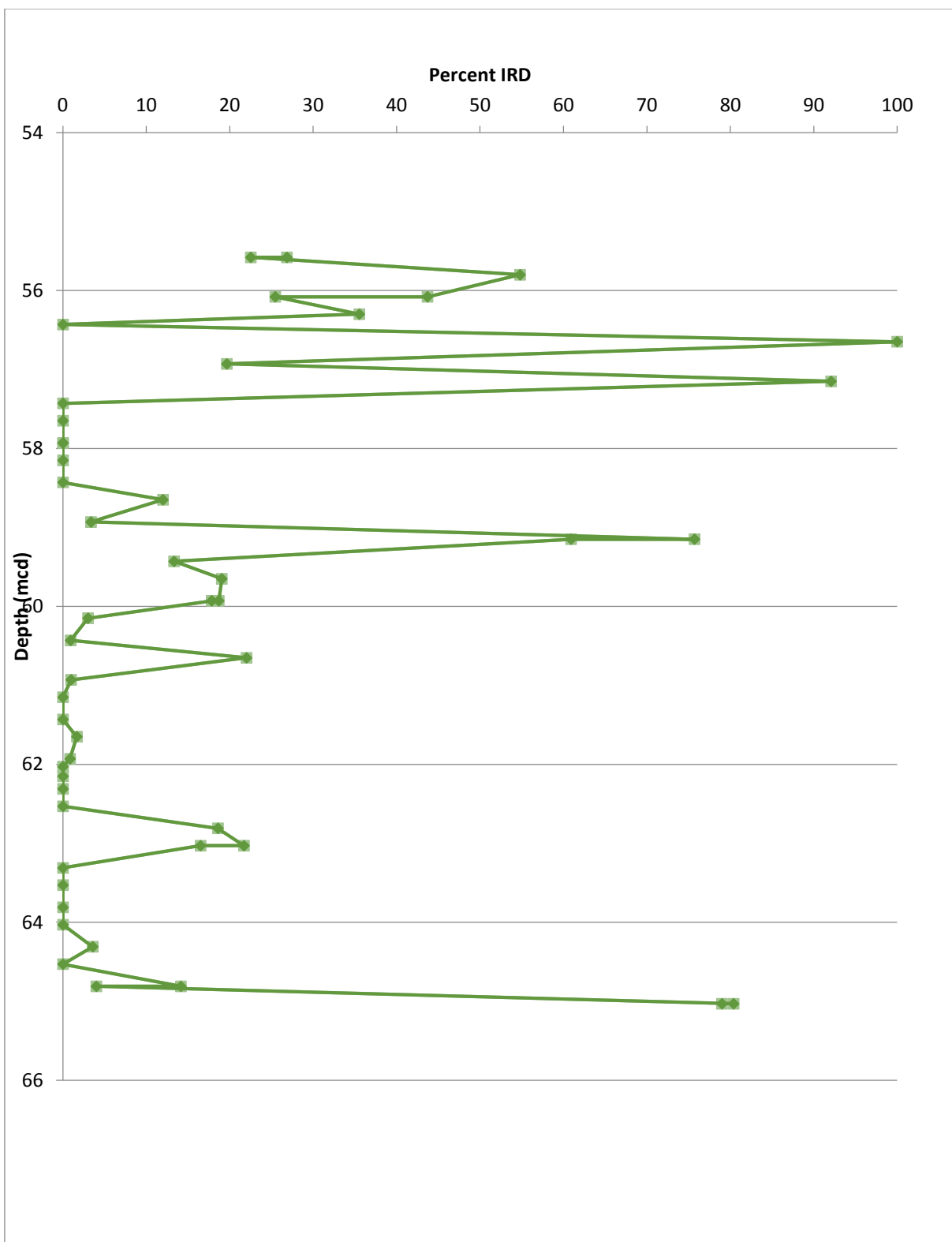


Figure 2: Abundance of terrestrial grains in sample in relation to composite core depth.

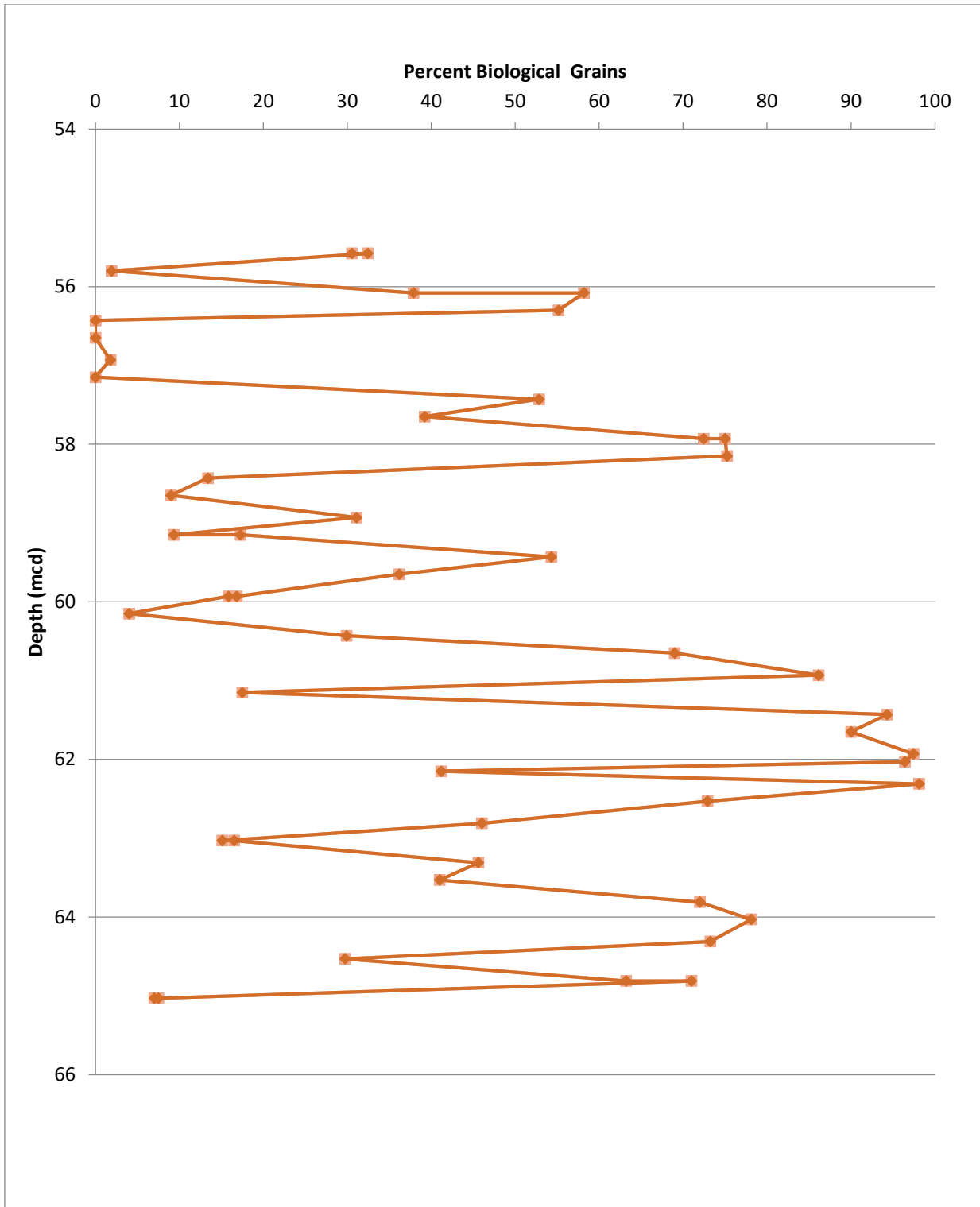


Figure 3: Abundance of biological grains in sample in relation to composite core depth.

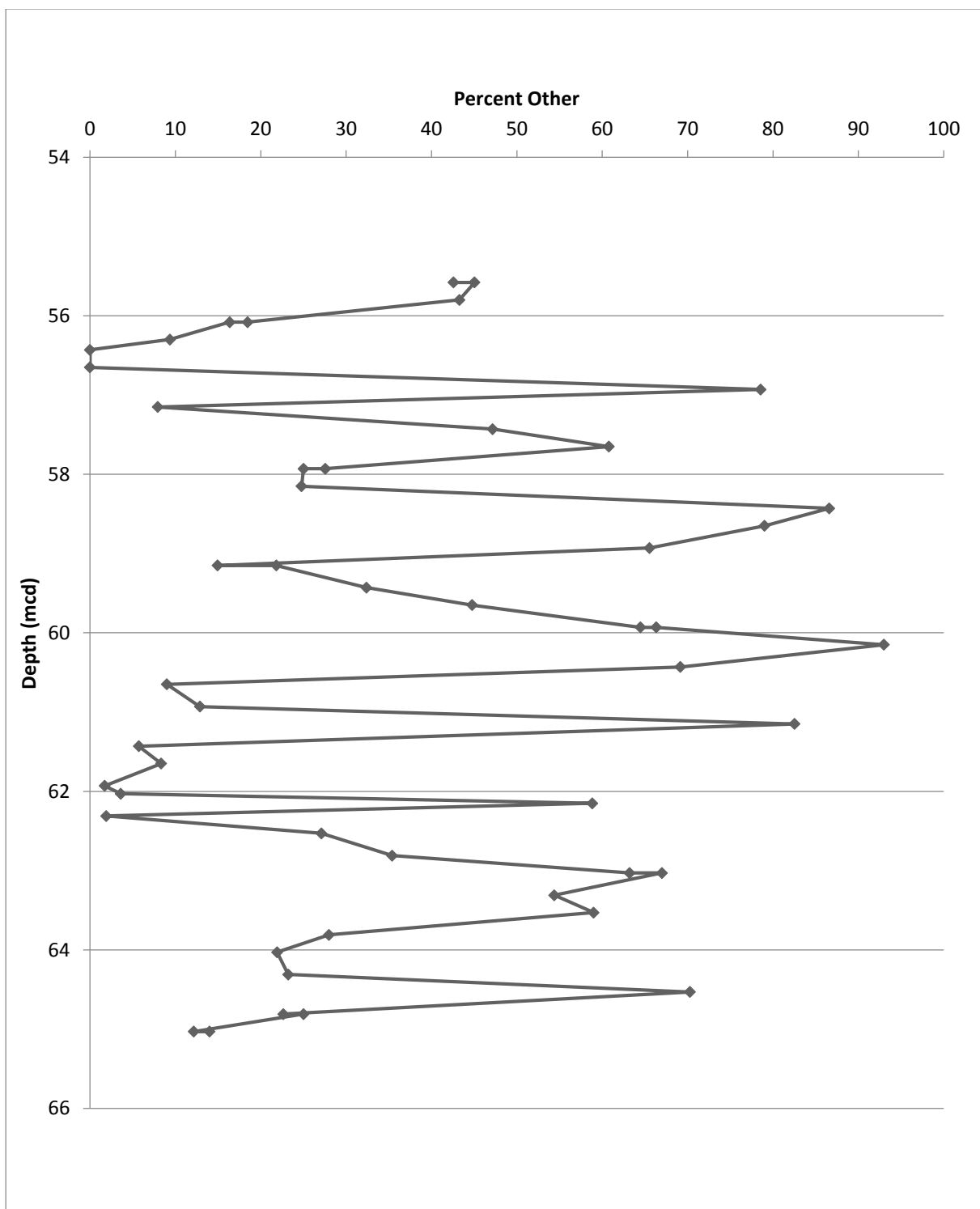


Figure 4: Abundance of other grains in sample in relation to composite core depth.

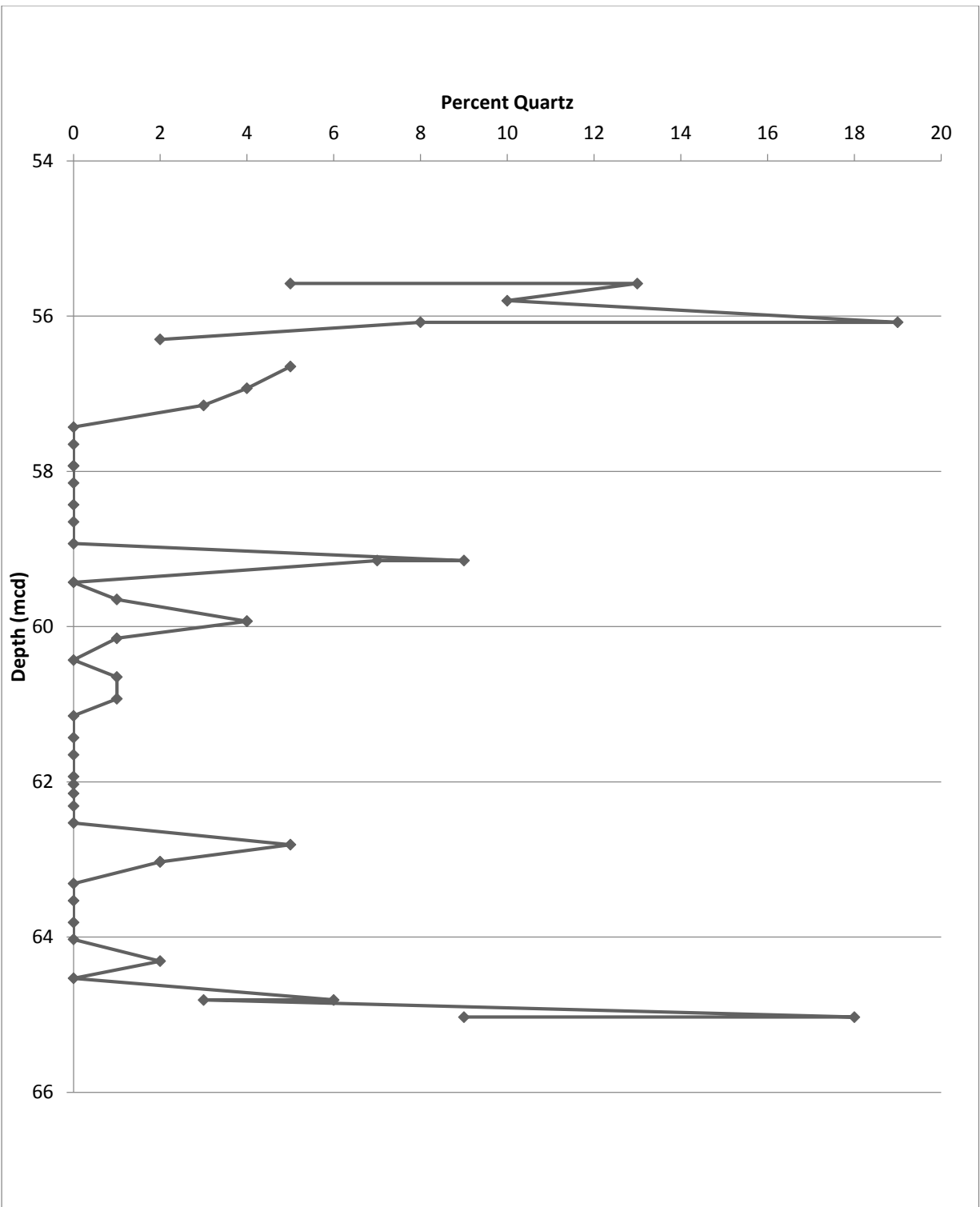


Figure 5: Abundance of quartz grains in sample in relation to composite core depth.

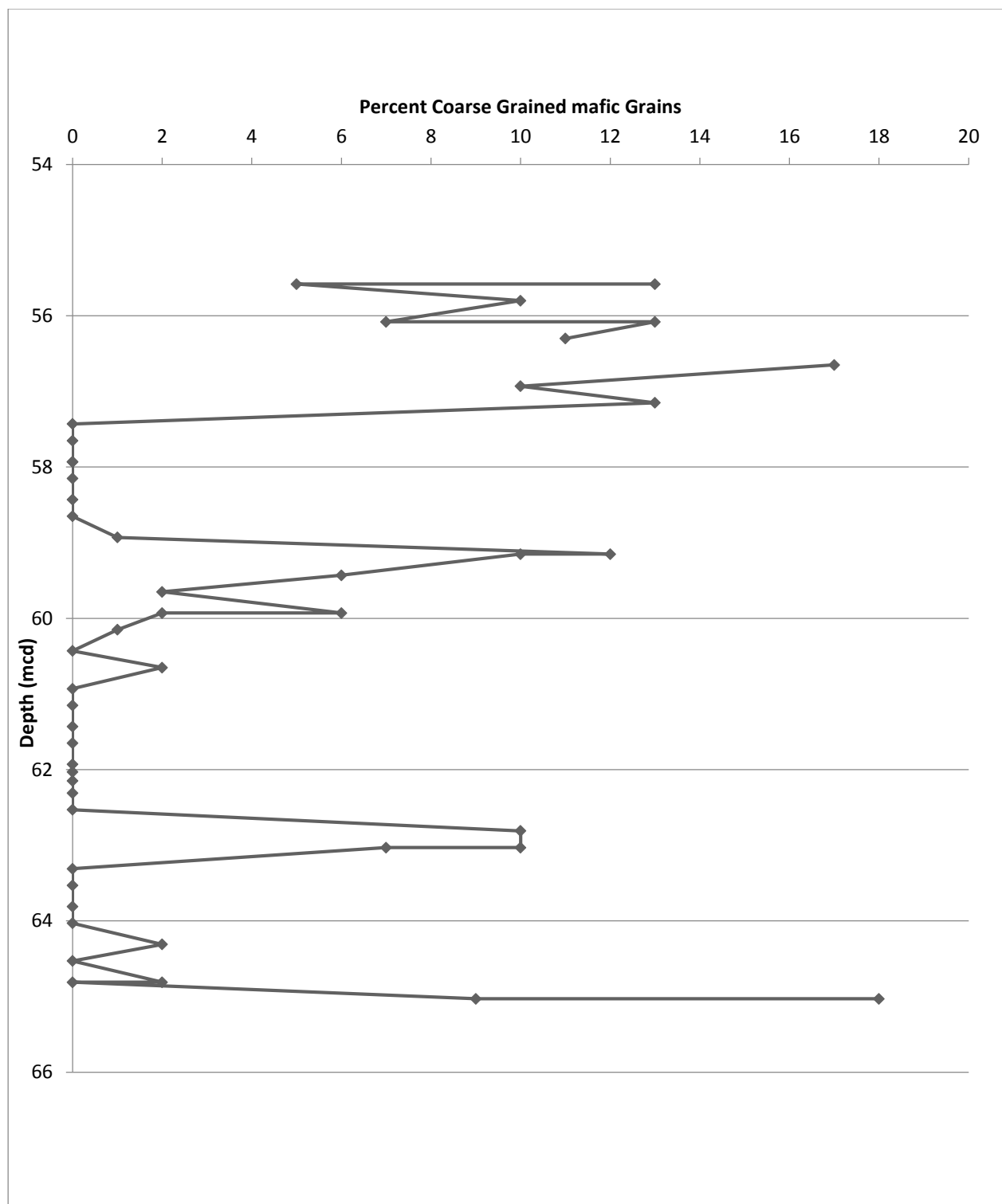


Figure 6: Abundance of coarse grained mafic grains in sample in relation to composite core depth.

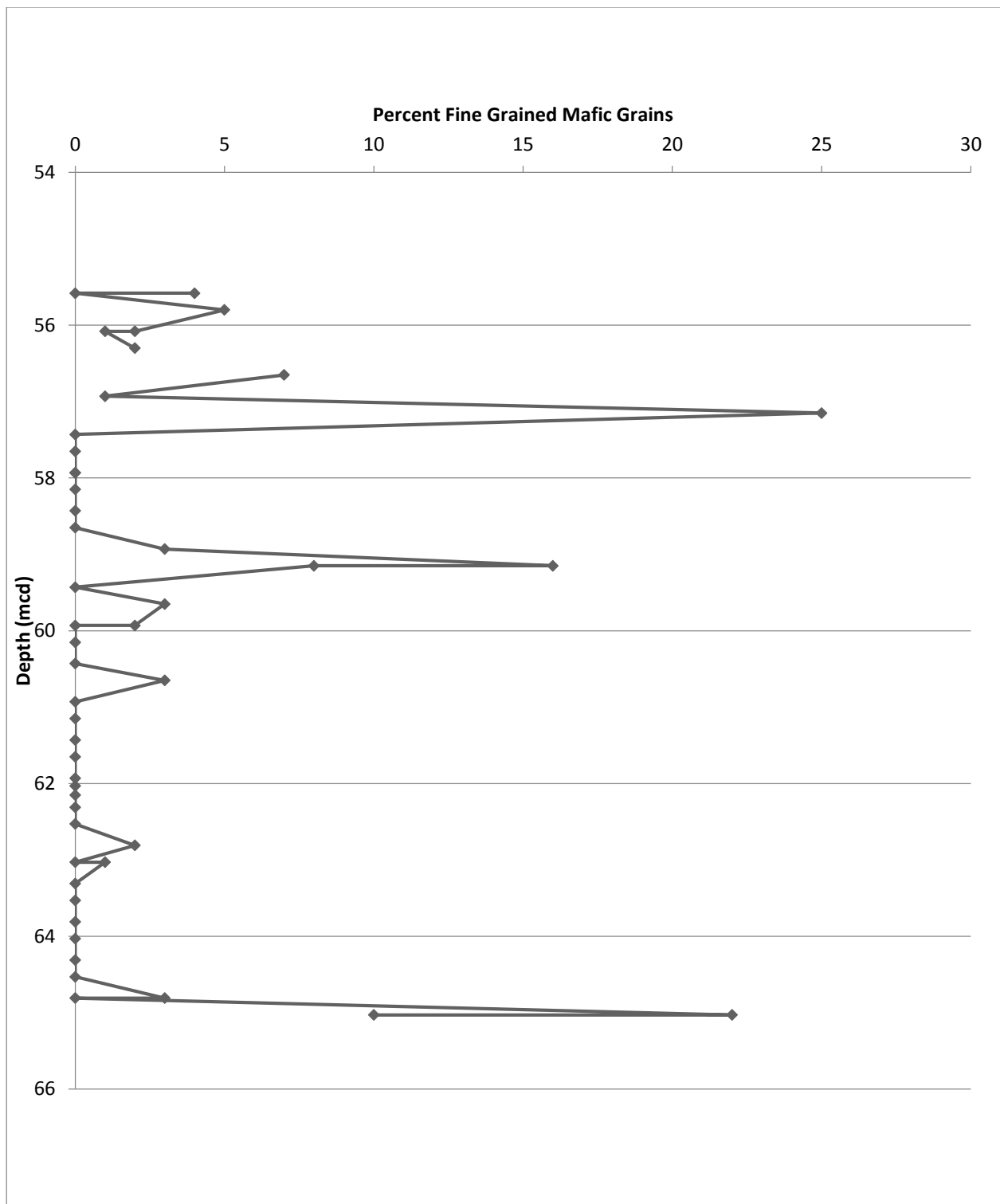
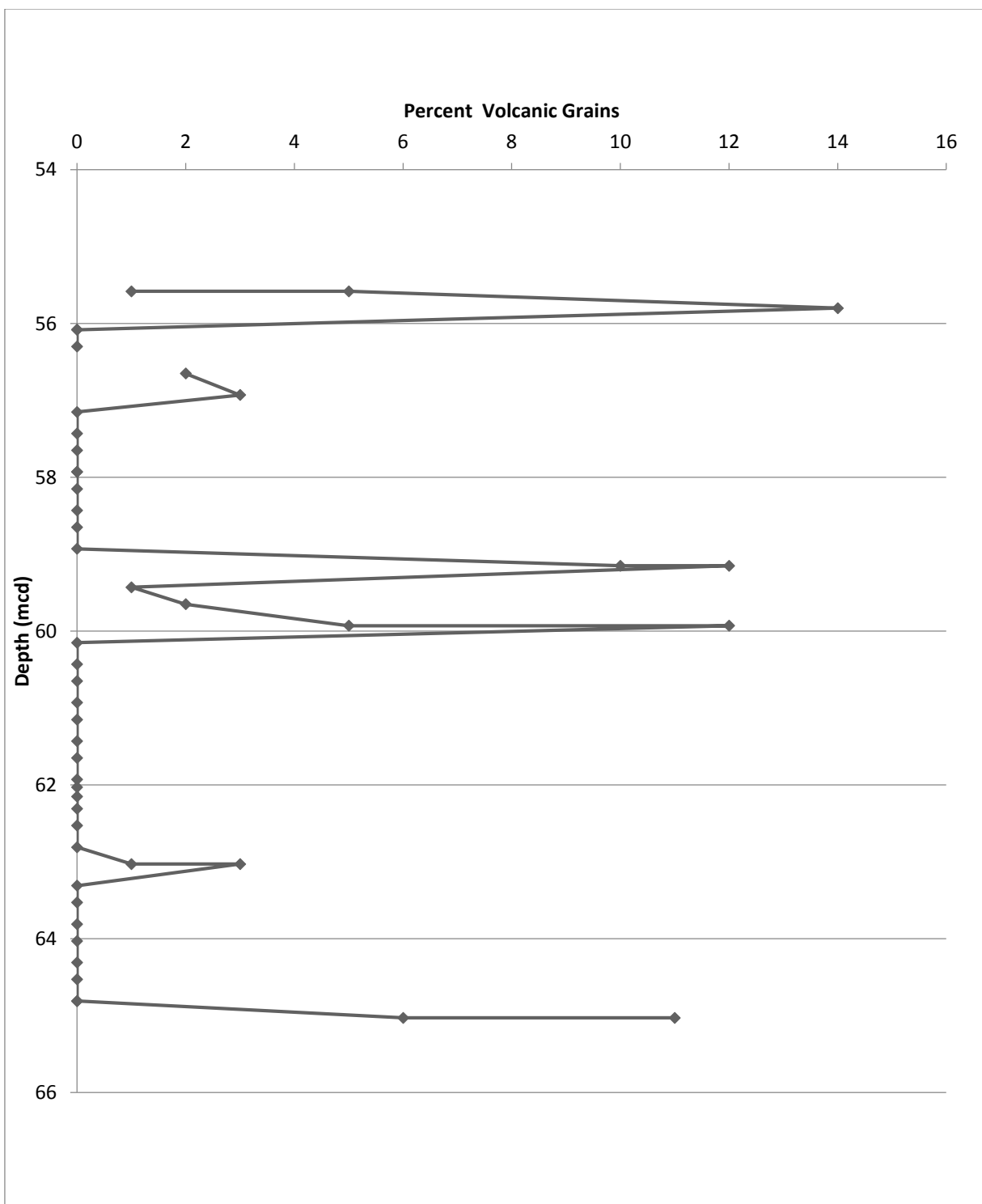


Figure 7: Abundance of fine grained mafic grains in sample in relation to composite core depth.



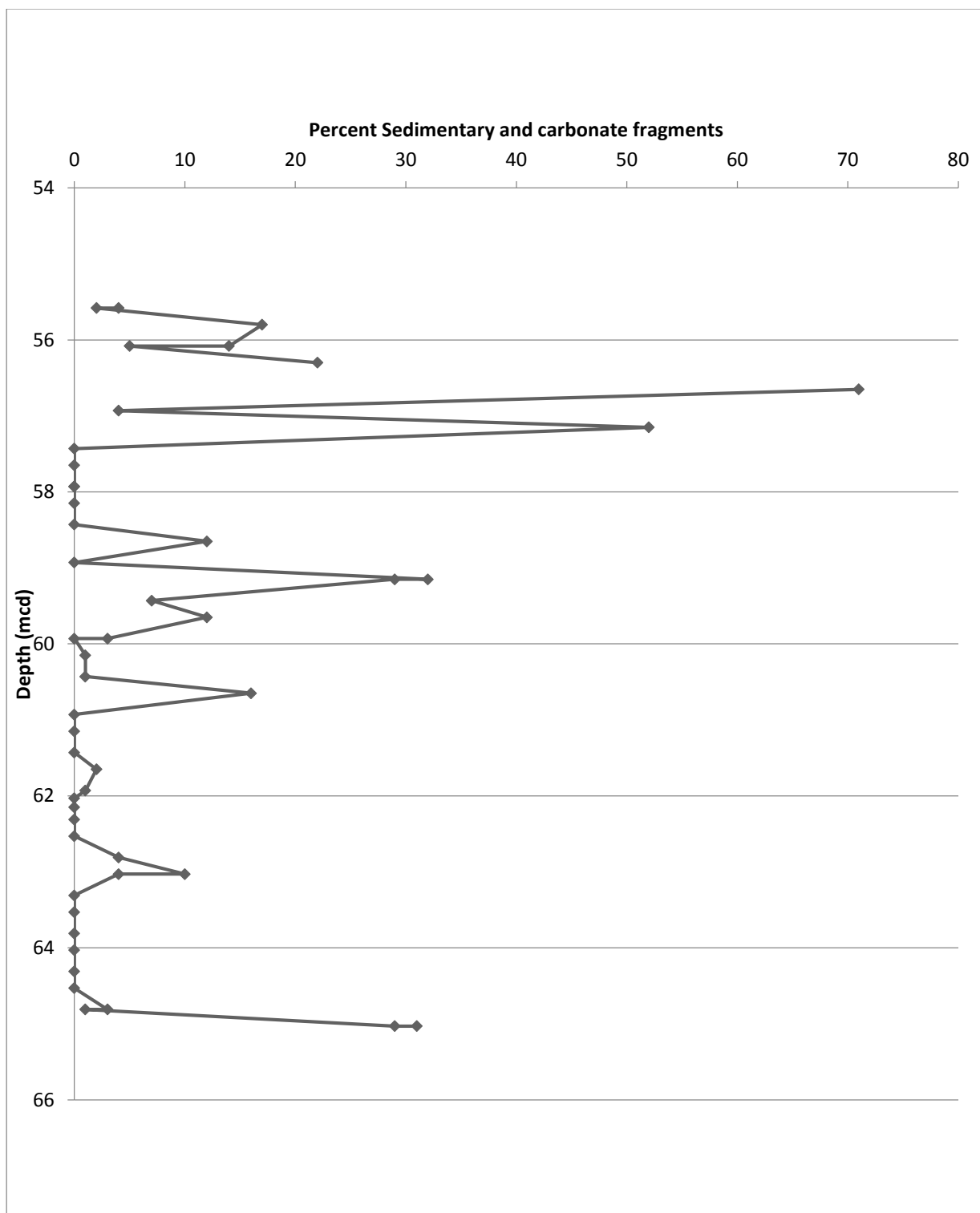


Figure 9: Abundance of sedimentary and carbonate fragment grains in sample in relation to composite core depth.

grain types exhibit a highly irregular pattern of grain abundances downcore. An example of this is Figure 4, which shows mudball abundances downcore. In contrast, the abundance patterns of some other grain types contain discrete intervals with consistently higher or lower values. This can be seen in Figure 2 which shows the abundance of total terrestrial grains (i.e., IRD).

The abundance data were then plotted against age; these plots are included in Appendix B. The record of glacial/interglacial stages (based on age data from Hodell et al. (2008) and glacial/interglacial stage data from Aitken & Stokes (1997)) was then overlain on the plots of grain abundances vs. age (Figures 10–17). Table 4, shown below, summarizes the record of glacial/interglacial data used. The age range calculated for this sample set was 851.5 to 969.625 kya which corresponds with mid Stage 21 (interglacial) through mid Stage 27 (interglacial).

MIS Stage and Age
Stage 21 (IG) is 866-814 ka
Stage 22 (Glacial) is 900 - 866 ka
Stage 23 (IG) is 917-900 ka
Stage 24 (Glacial) is 936-917 ka
Stage 25 (IG) is 959 - 936 ka
Stage 26 (Glacial) is 970-959 ka
Stage 27 (IG) is 982-970 ka
982

Table 3: Aitken& Stokes (1997) glacial/interglacial stage data

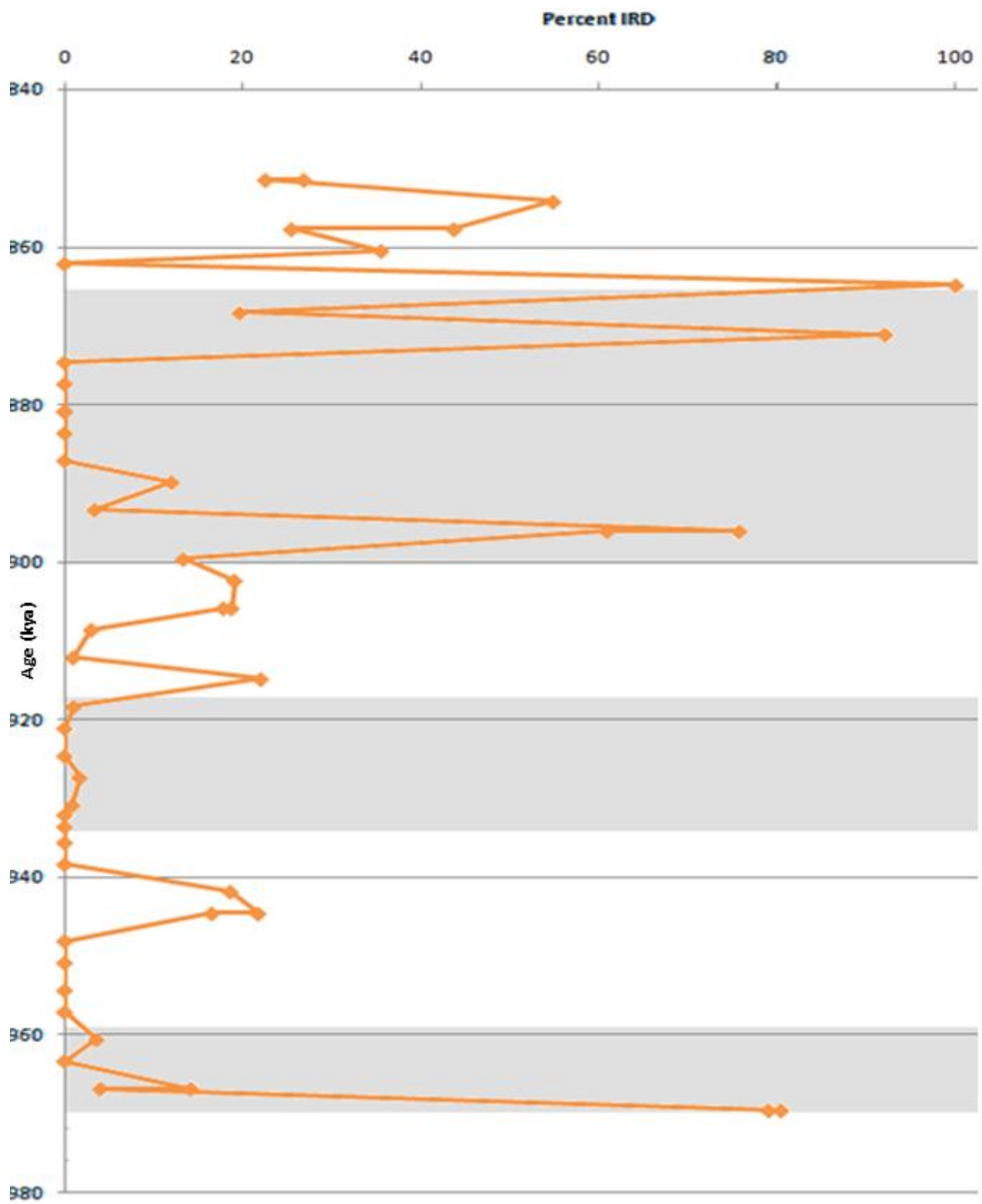


Figure 10: Abundance of total terrestrial grains in relation to age with included glacial (grey shaded areas) and interglacial (areas with no shading) periods.

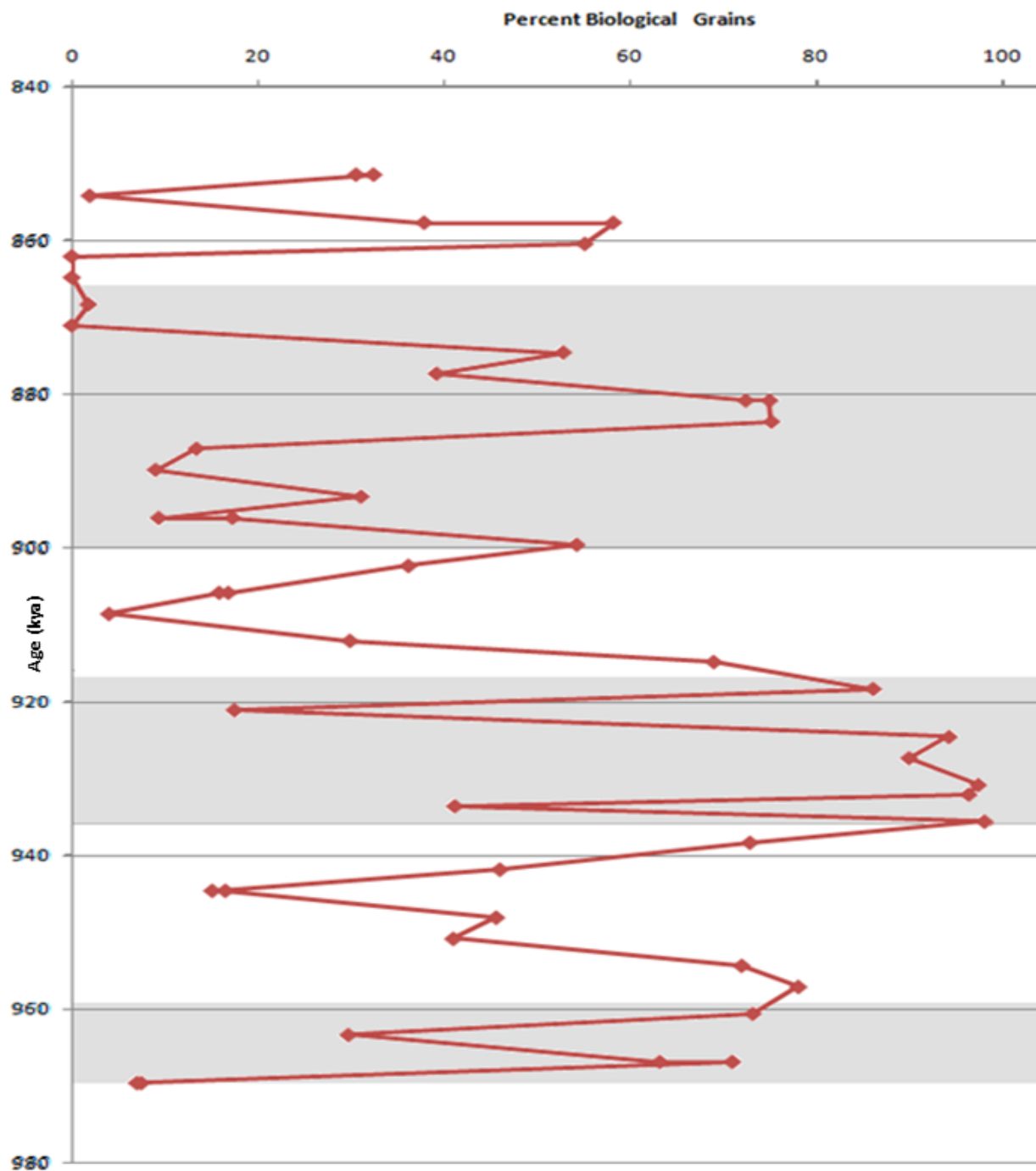


Figure 11: Abundance of total biological grains in relation to age with included glacial (grey shaded areas) and interglacial (areas with no shading) periods.

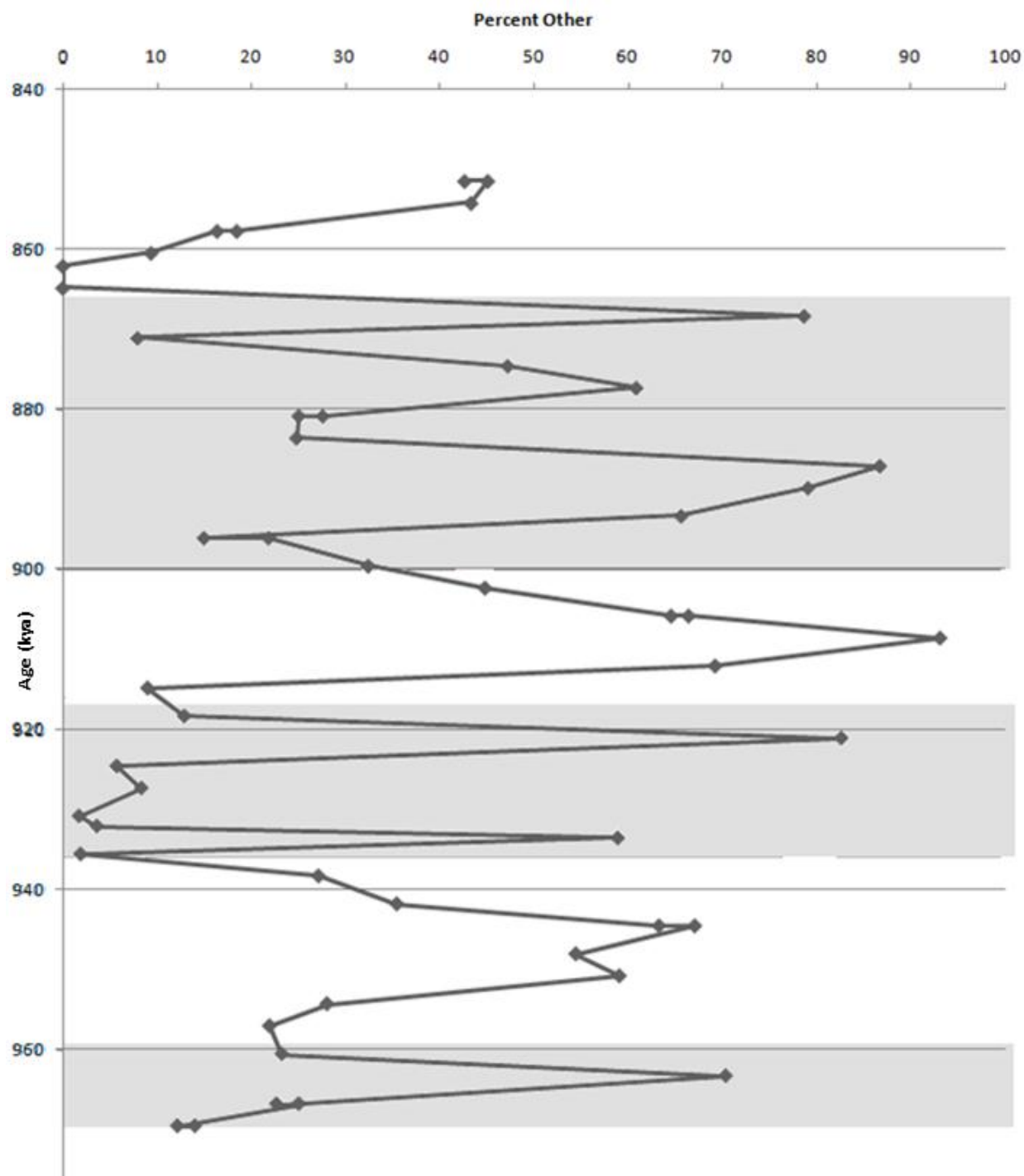


Figure 12: Abundance of total other grains in relation to age with included glacial (grey shaded areas) and interglacial (areas with no shading) periods.

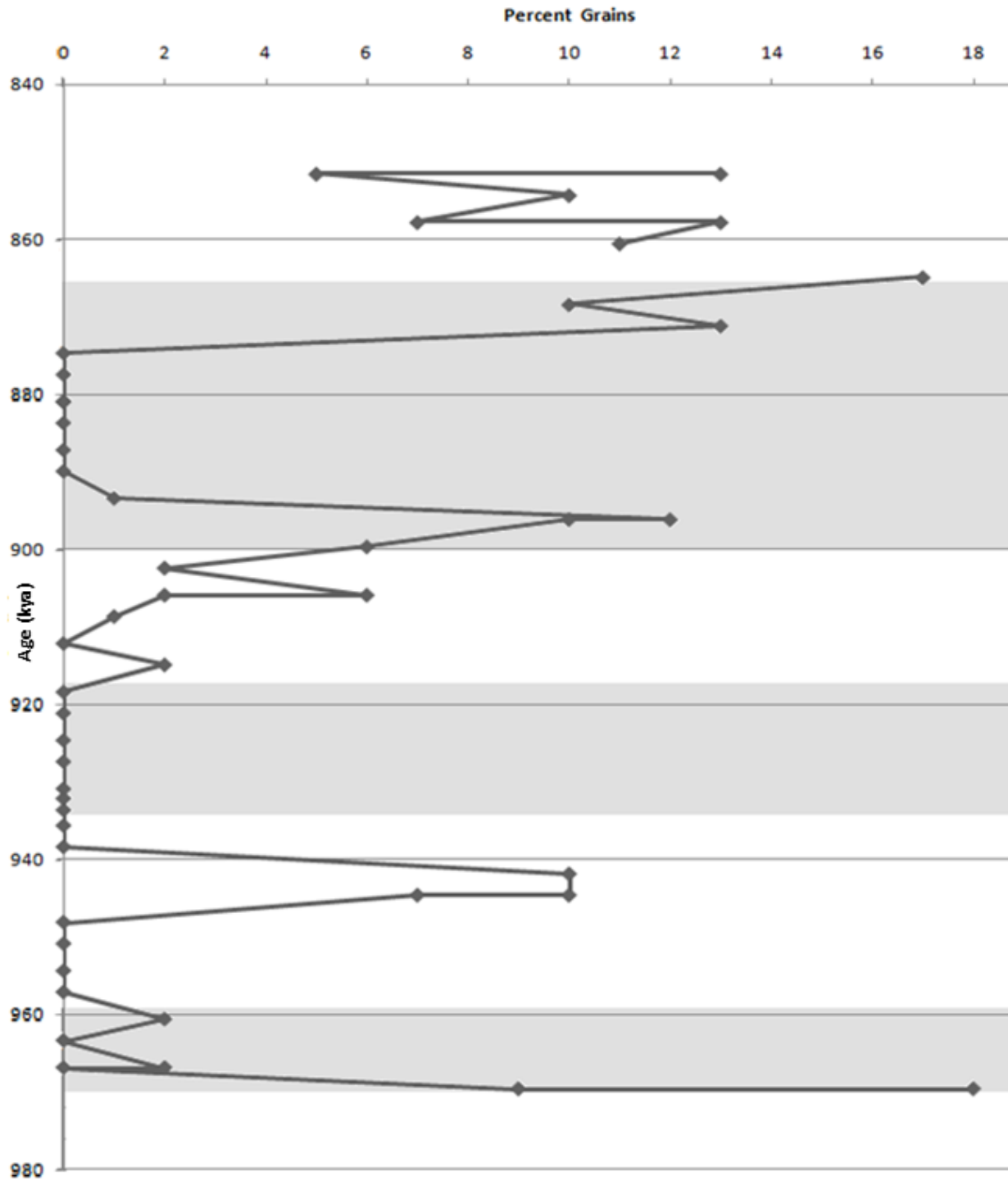


Figure 13: Abundance of total coarse grained mafic grains in relation to age with included glacial (grey shaded areas) and interglacial (areas with no shading) periods.

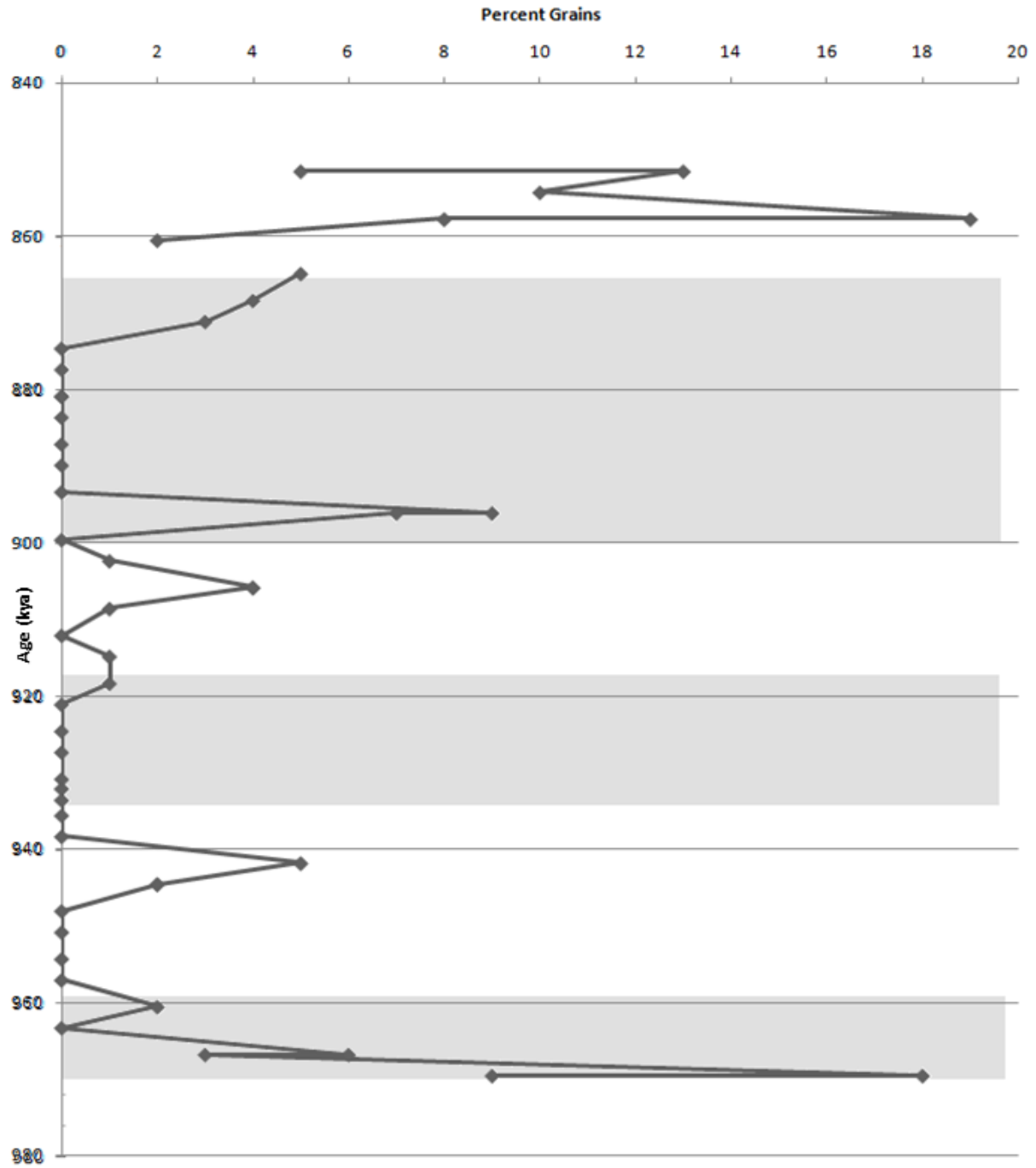


Figure 14: Abundance of total quartz grains in relation to age with included glacial (grey shaded areas) and interglacial (areas with no shading) periods

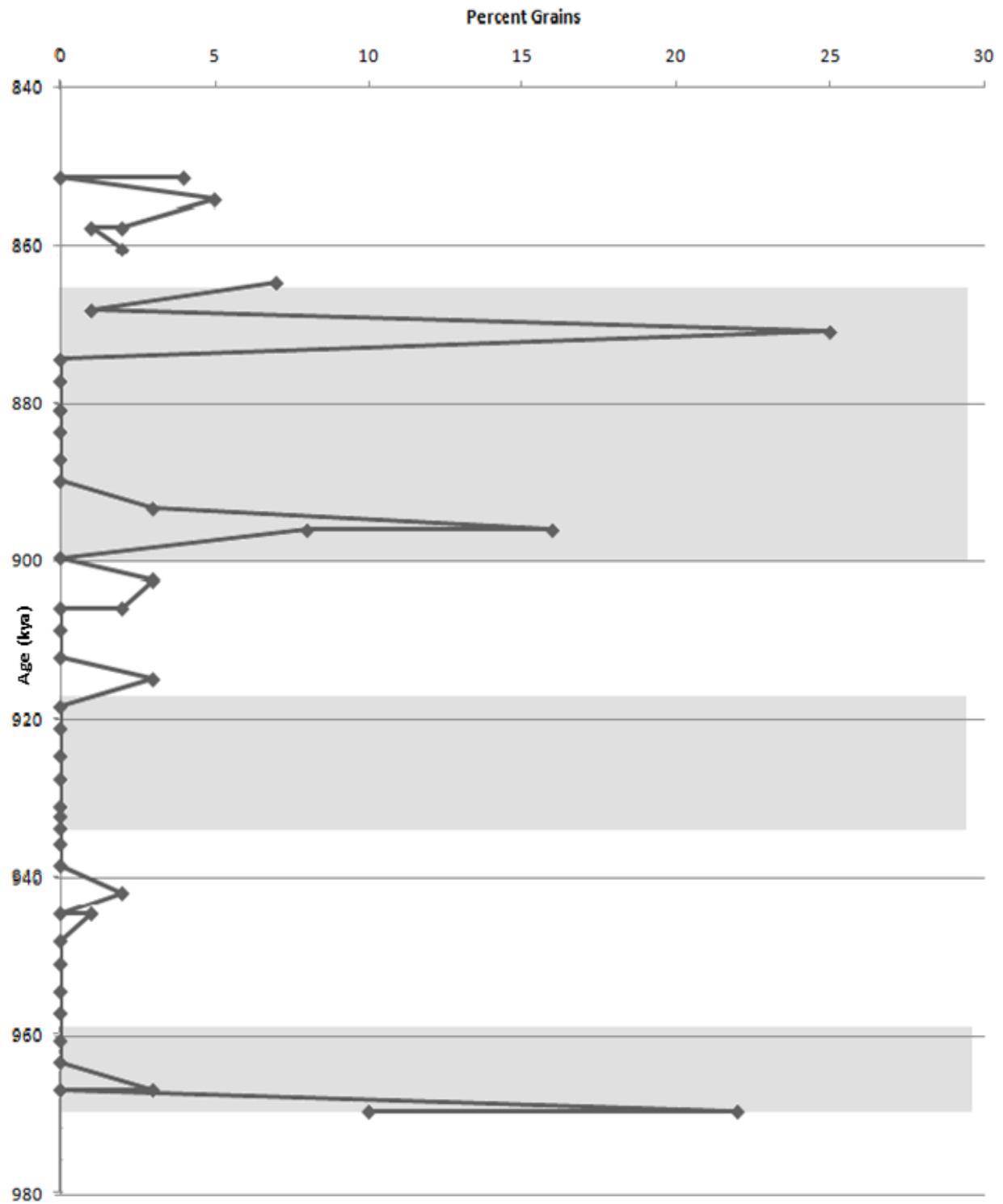


Figure15: Abundance of total fine grained mafic grains in relation to age with included glacial (grey shaded areas) and interglacial (areas with no shading) periods

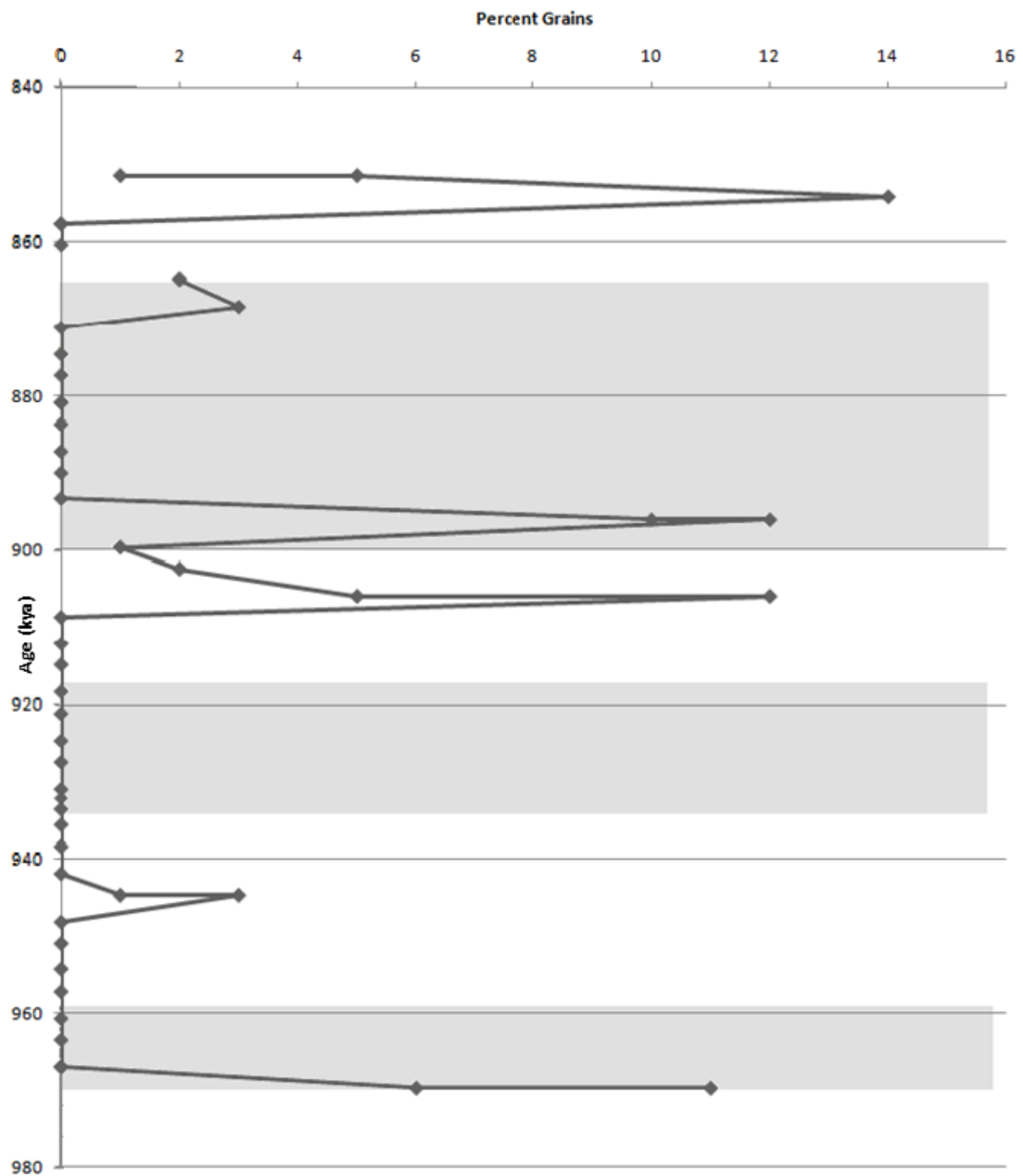


Figure 16: Abundance of total volcanic grains in relation to age with included glacial (grey shaded areas) and interglacial (areas with no shading) periods

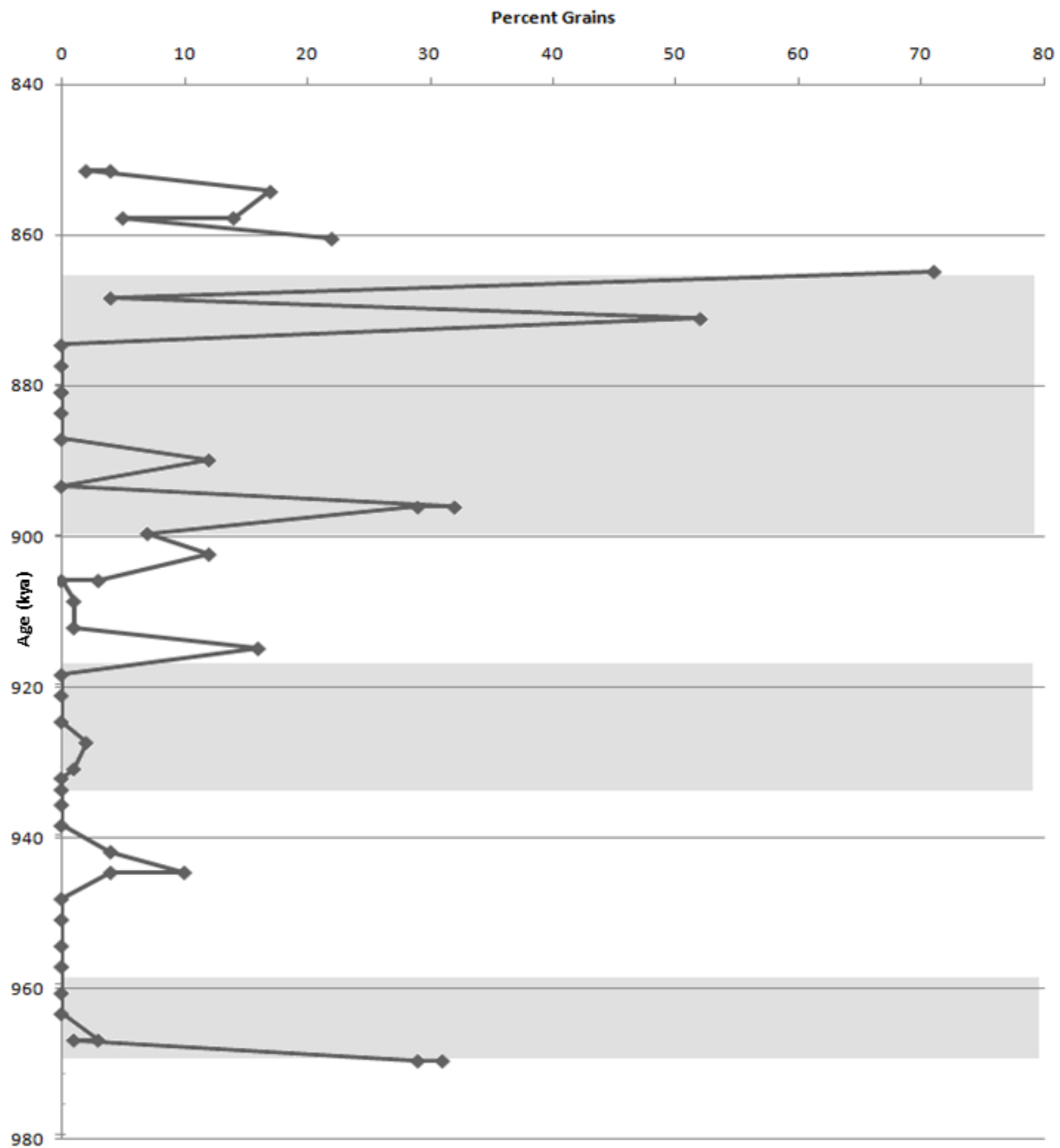


Figure 17: Abundance of total sedimentary and carbonate fragment grains in relation to age with included glacial (grey shaded areas) and interglacial (areas with no shading) periods

Discussion

Because mudballs are an artifact of sample preparation, rather than a primary grain type, their high average abundance and variations introduce a variable dilution effect on the abundances of the terrestrial and biogenic primary grains. In order to remove this dilution effect the abundances of the terrestrial and biogenic grains have been recalculated on a mudball-free basis; those abundance plots are shown in Figures 18–25.

The data acquired from this sample set show major variations in grain abundances through time. These include a high average abundance of mudballs, with major abundance variations. The mudball-free total terrestrial (IRD) data (Figures 18 & 25) primarily show abundance peaks at the transitions between glacial and interglacials and within interglacials. In contrast, total terrestrial abundances, tend to be low in the middle of a glacial stage. A possible reason for this pattern is that during glacial expansion, ice transported the more easily eroded debris that had weathered during the previous interglacial stage (St. John et al., 2004). This would have caused a large influx of ice rafted debris at the start of a glacial stage. The low abundances of ice rafted debris within the centers of the glacial stages may reflect either a glacial change to a cold-based regime, or the presence of sea ice that repressed iceberg movement. The increased abundances of ice rafted debris at the end of a glacial stage could reflect a transition from dry-based to wet-based ice, and to an overall decrease in glacial volume thereby increasing the transport of terrestrial debris. The biological grain abundances are

inversely proportional to the terrestrial grain abundances, as is required for the mudball-free data by the presence of only two grain types (terrestrial and biologic).

The provenance of IRD grain types in the North Atlantic has been studied previously, and source areas for each have been identified (Krissek & St. John, 2004). The IRD grain abundances shown in Figures 20–24 indicate that sedimentary/carbonate rock fragments, quartz, and mafic grains are the most abundant grain types. As a result, the majority of ice rafted debris is likely to have originated from Iceland (mafics), Greenland (mafics and quartz) and Canada (quartz and sedimentary/carbonate rock fragments) at roughly equal rates. The higher abundances of quartz and sedimentary/ carbonate rock fragments within the IRD from ~927 kya to ~912 kya suggest an increased IRD supply from Canada and possibly southern Greenland during that time. This may indicate differences in timing and/or style of transition into the interglacial stage for different source areas. An increase in the volcanic grain abundances at ~905.4 kya suggests an increase in volcanic activity within the region at that time. The most likely source is Iceland, although more research is needed in order to pinpoint a specific area or event.

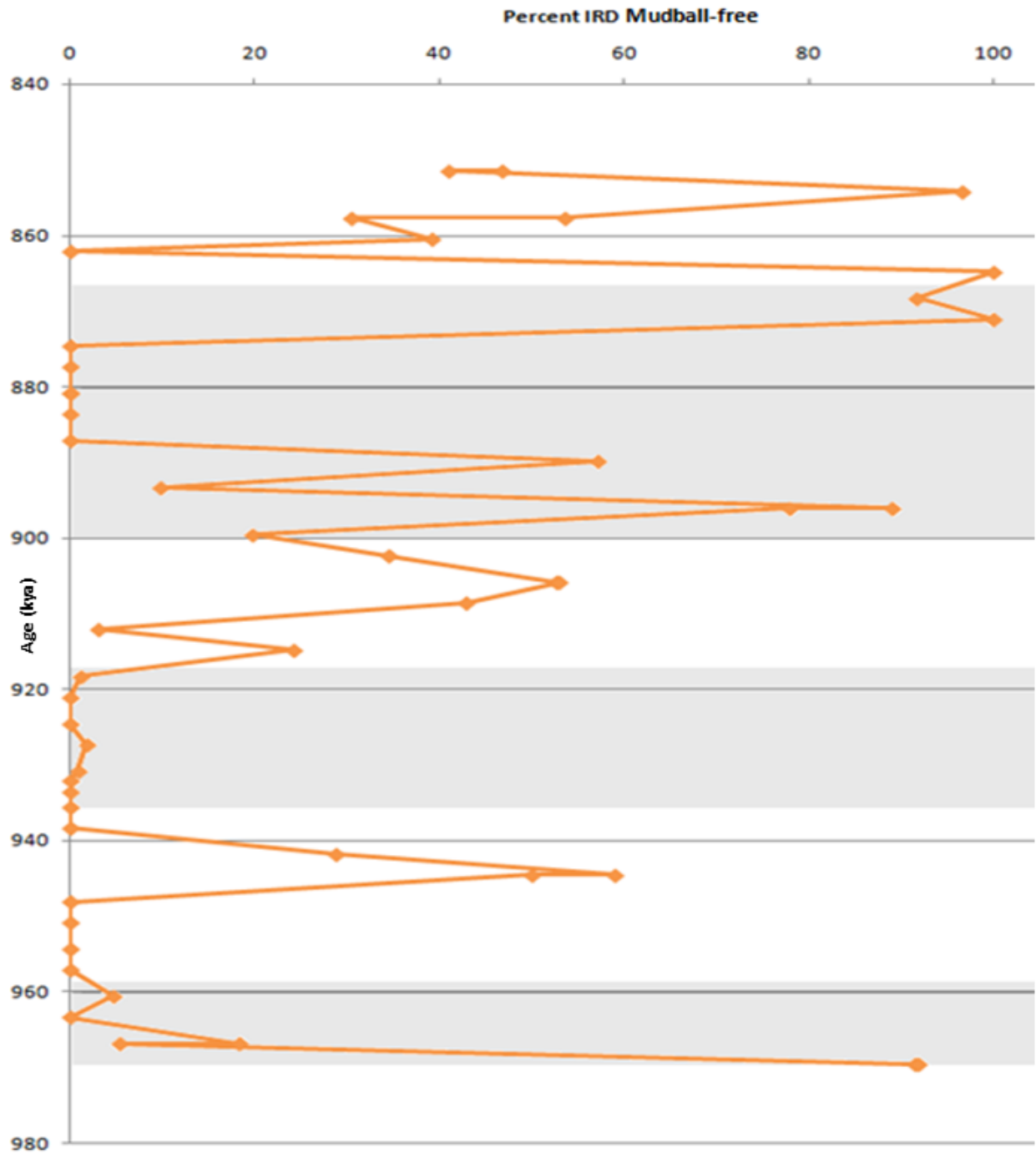


Figure 18: Abundance of total terrestrial grains in relation to age with included glacial (grey shaded areas) and interglacial (areas with no shading) periods. This data set is calculated on a mudball-free basis.

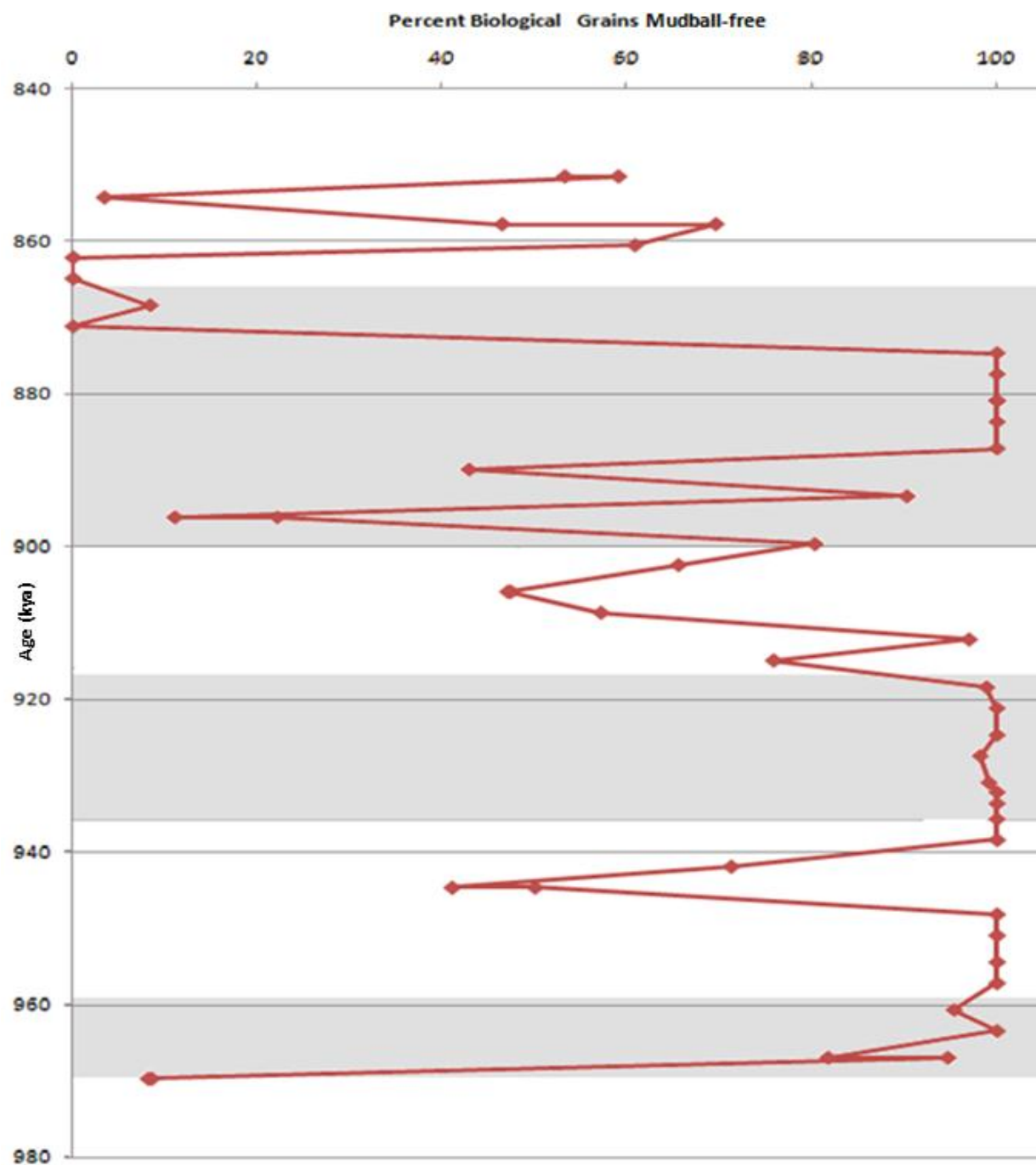


Figure 19: Abundance of total biogenic grains in relation to age with included glacial (grey shaded areas) and interglacial (areas with no shading) periods. This data set is calculated on a mudball-free basis.

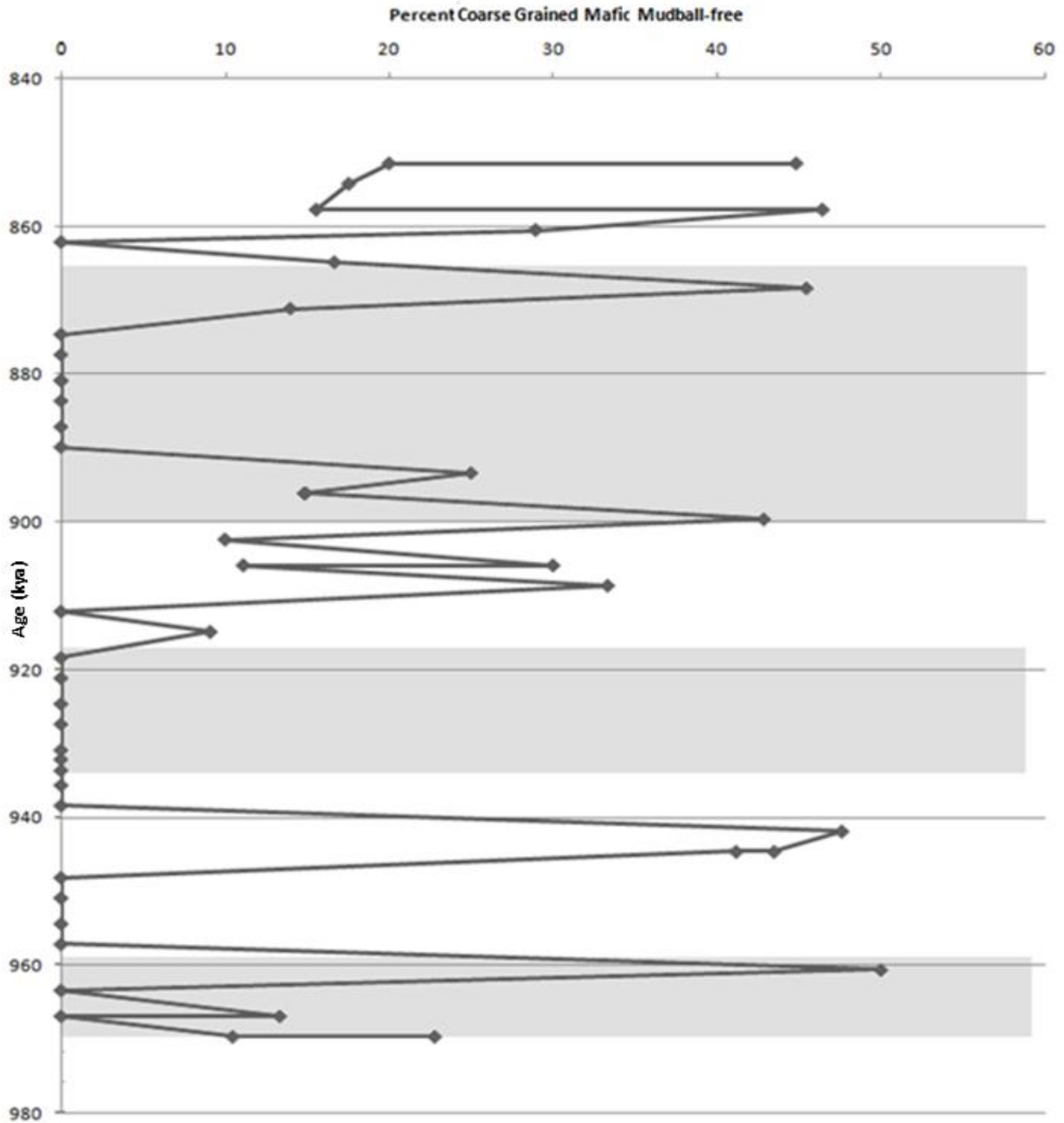


Figure 20: Abundance of total coarse grained mafic grains in relation to age with included glacial (grey shaded areas) and interglacial (areas with no shading) periods. This data set is calculated on a mudball-free basis.

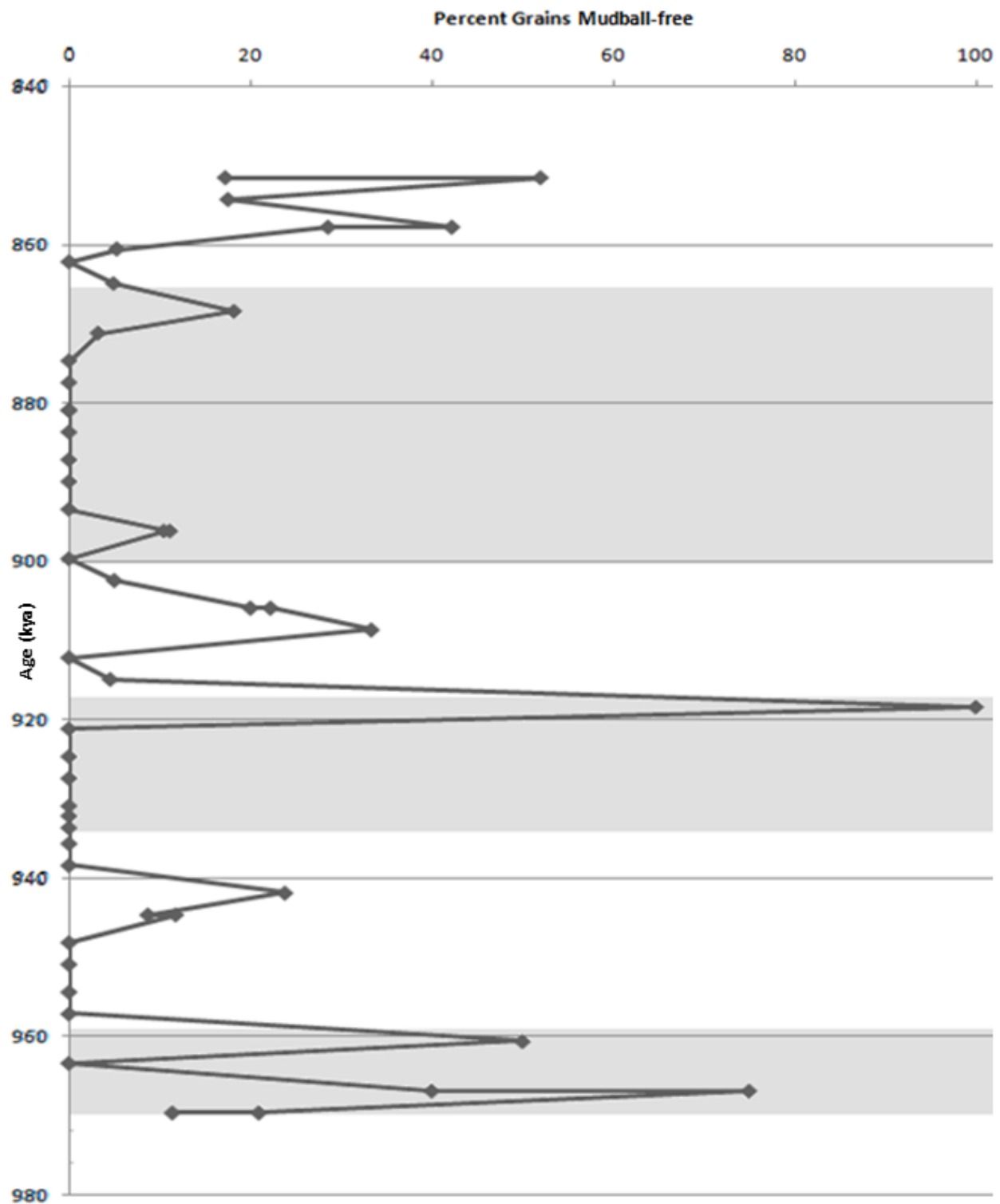


Figure 21: Abundance of total quartz grains in relation to age with included glacial (grey shaded areas) and interglacial (areas with no shading) periods. This data set is calculated on a mudball-free basis.

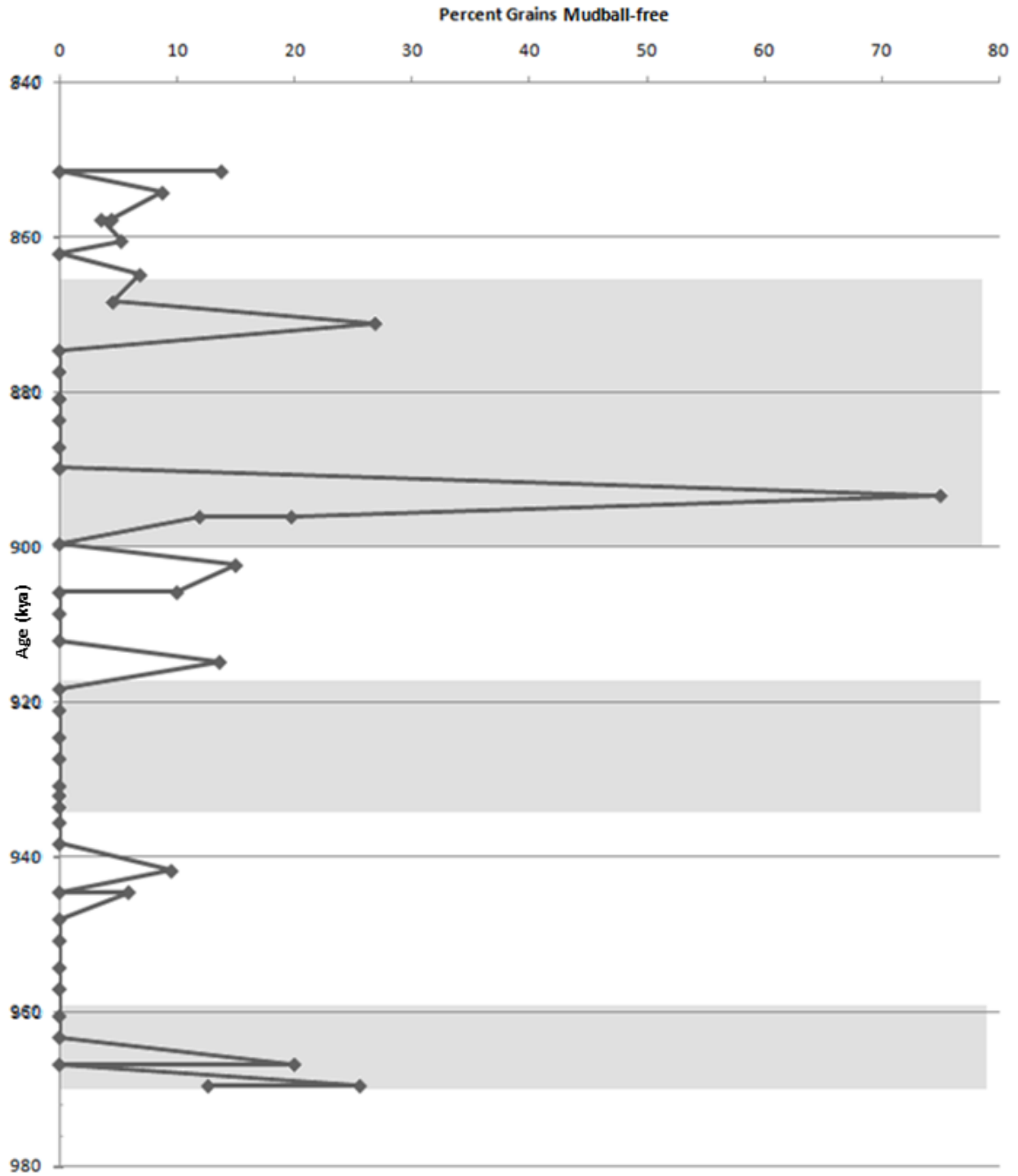


Figure 22: Abundance of total fine grained mafic grains in relation to age with included glacial (grey shaded areas) and interglacial (areas with no shading) periods. This data set is calculated on a mudball-free basis.

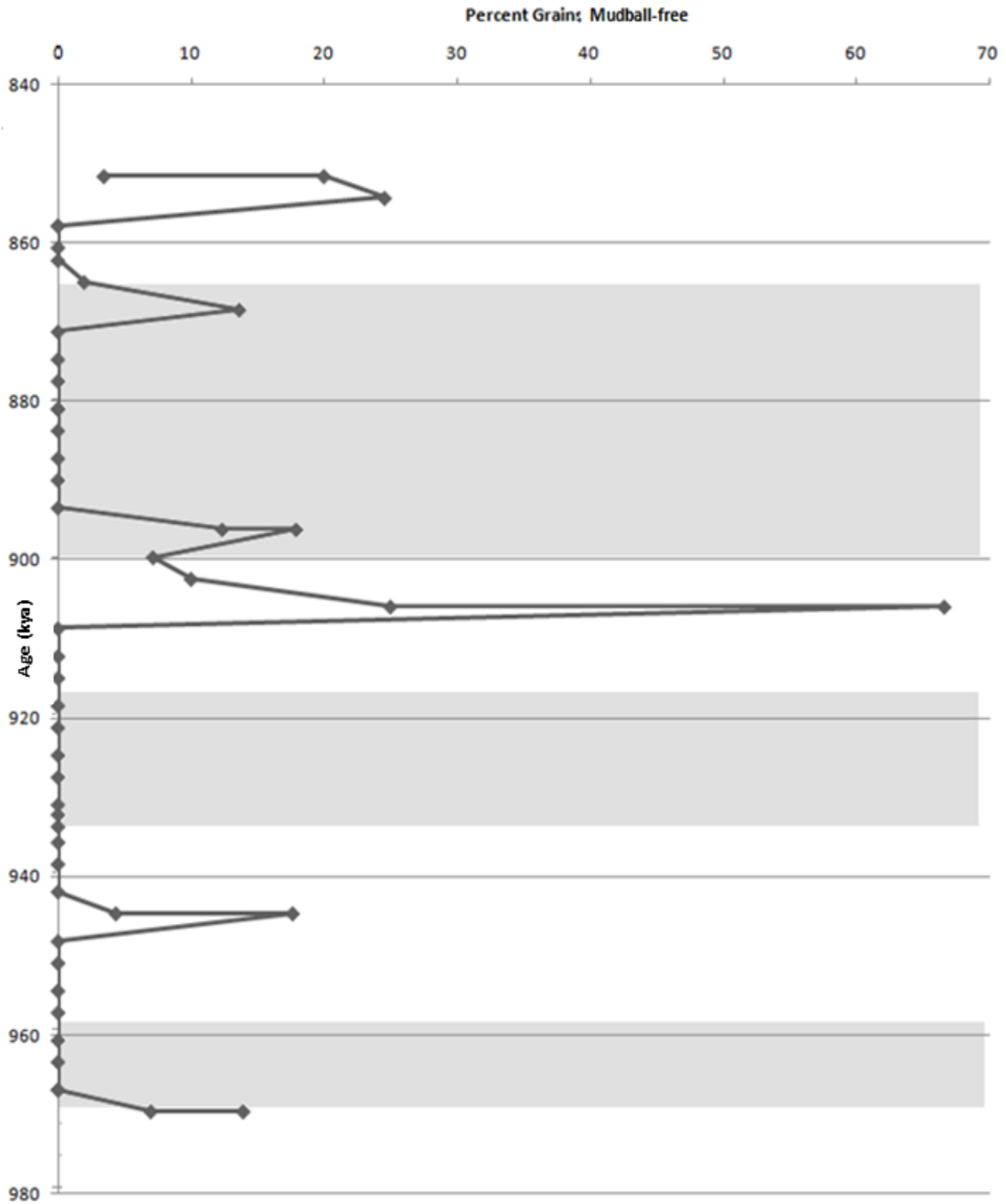


Figure 23: Abundance of total volcanic grains in relation to age with included glacial (grey shaded areas) and interglacial (areas with no shading) periods. This data set is calculated on a mudball-free basis.

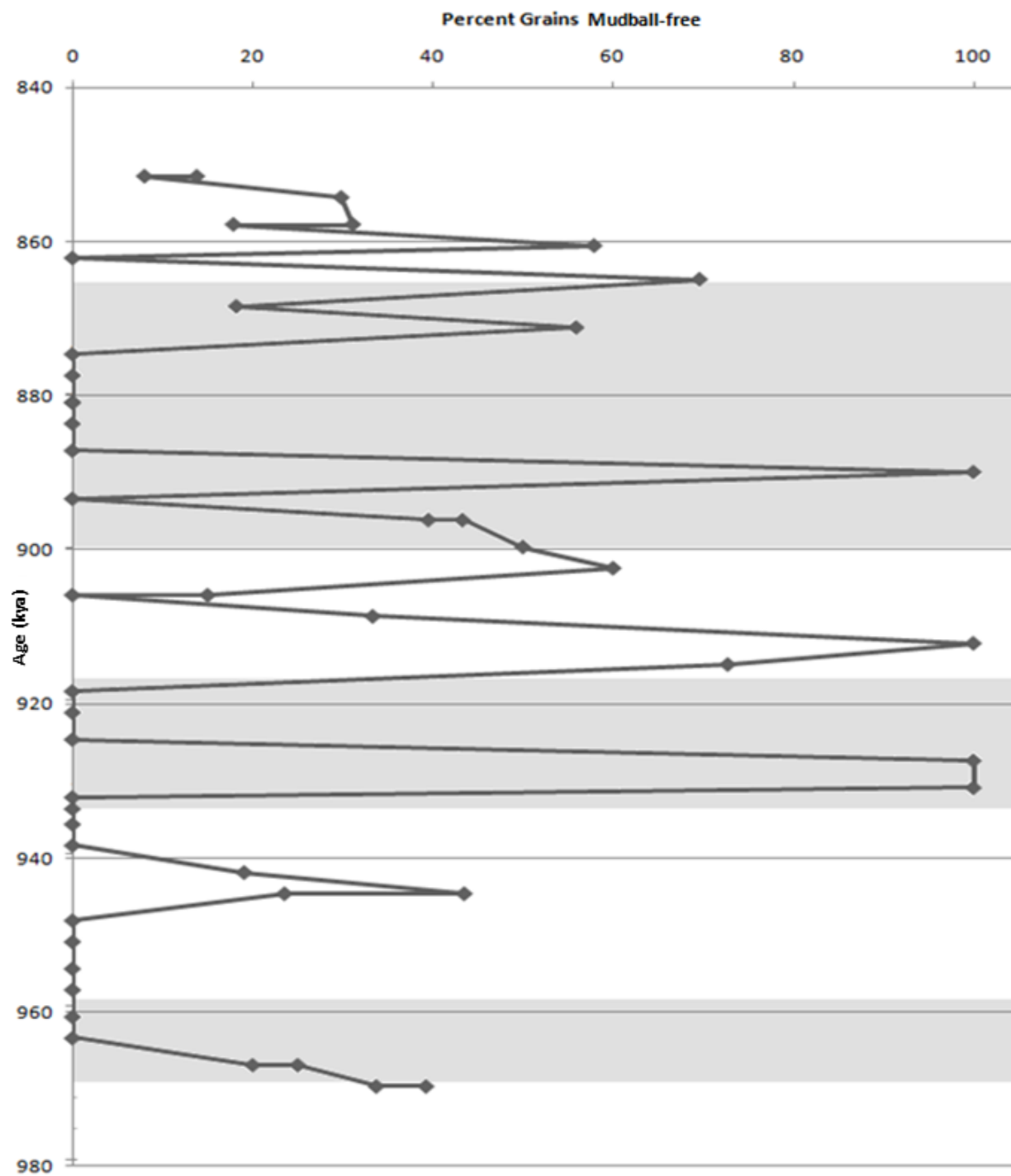


Figure 24: Abundance of total sedimentary and carbonate fragment grains in relation to age with included glacial (grey shaded areas) and interglacial (areas with no shading) periods. This data set is calculated on a mudball-free basis.

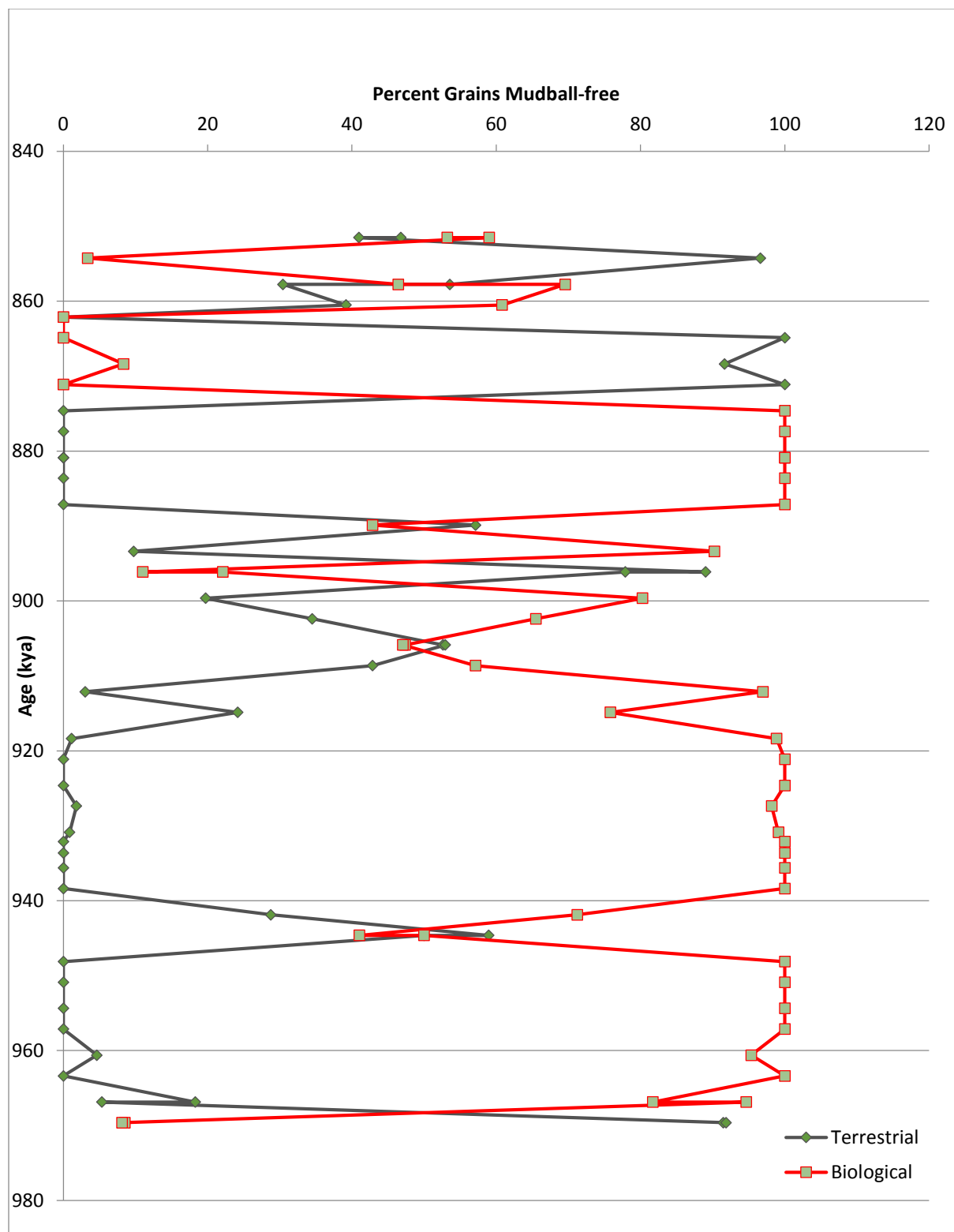


Figure 25: Percent terrestrial and biological grains in relation to age. This data set is without 'other' grain dilution.

Conclusions

Grain counts of the medium to coarse sand fraction of samples from Site 1308 have provided information about grain compositions and abundances. Grains were classified into three main categories: Terrestrial, Biological, and Other. The composition of the ice rafted debris was determined by identifying the lithologies of the terrestrial grains. These data span the interval from 851.5 kya to 969.625kya and include several glacial/interglacial cycles. When the diluting effects of non-primary grains were removed, it was found that terrestrial grain abundances generally peak near glacial/interglacial transitions. This is interpreted to result from changing climatic, glacial, and oceanographic conditions that restricted or enhanced the flow/transit of ice. In general, increases in the total IRD abundance were caused by increased abundances of multiple IRD grain types, suggesting relatively synchronous changes in IRD supply from multiple source areas. The relative importance of quartz and sedimentary/carbonate IRD increased significantly at 927 kya to 912 kya, however, indicating a major increase in IRD supply from Canada/southern Greenland at that time. A spike in volcanic activity at 905.4 kya is suggested by an increase in volcanic IRD at that time.

Recommendations for Future Work

There are several ways the grain census process could be improved. Better care to clean and label the samples could be implemented. Some of the

samples studied were labeled incorrectly and several of the samples examined were completely, or nearly completely, composed of mudballs. Possibly extending the length or number of times the sample is run through the ultrasonic bath could reduce the number of mudballs within the sample. Other methods could also be used to concentrate the terrestrial grains, such as the use of acids to dissolve biological grains, or even the use of heavy-liquid separations. This would allow a more accurate count and would eliminate dilution of the terrestrial grains. An additional sieving step could also help to remove many of the smaller forams and mudballs.

Expansion of the research area would also be helpful for improving the extent and accuracy of this project. Further study of older sediments would enhance our knowledge of the paleoclimate in the North Atlantic and provide information on past climate changes. Additional samples taken from nearby locations would help improve the accuracy of this research, and correlation to results from cores worldwide would give us a global picture. Supplementary research could also be done regarding the exact Nd, Sr and Pb isotopic compositions of the IRD in order to better determine the precise provenance for the terrestrial grains (Farmer et al., 2003).

References Cited

- Aitken, Martin J., and Stephen Stokes. (1997), *Climatostratigraphy. Chronometric Dating in Archaeology*. Springer US, 1-30.
- Alley, R., Cuffey, K., Evenson, E., Strasser, J., Lawson, D. and Larson, G., (1997), How Glaciers Entrain And Transport Basal Sediment: Physical Constraints, *Quaternary Science Reviews* 16.9. 1017-1038.
- De Schepper, S., M. J. Head, and J. Groeneveld (2009), North Atlantic Current variability through marine isotope stage M2 (circa 3.3 Ma) during the mid-Pliocene, *Paleoceanography*, 24, PA4206, doi: 10.1029/2008PA001725.
- Dowdeswell, Julian A., and Evelyn K. Dowdeswell. Debris In Icebergs And Rates Of Glaci-Marine Sedimentation: Observations From Spitsbergen And A Simple Model. *Journal of Geology* 97.2 (1989): 221-231.
- Farmer, G.Lang, Donald Barber, and John Andrews, (2003), Provenance Of Late Quaternary Ice-Proximal Sediments In The North Atlantic: Nd, Sr And Pb Isotopic Evidence, *Earth and Planetary Science Letters* 209, 1-2, 227-243.
- Hodell, David A., James E. T. Channell, Jason H. Curtis, Oscar E. Romero, and Ursula Röhl, (2008), Onset of “Hudson Strait” Heinrich Events in the Eastern North Atlantic at the End of the Middle Pleistocene Transition (~640 Ka)? *Paleoceanography*, 23.4
- Krissek, L.A., and St. John, K., (2002), Pleistocene iceberg production from East Greenland: synchronous between source areas, but distinct from global ice volume, *Bulletin of the Geological Society of Denmark*, 49, 79-89.
- St. John, Kristen, Benjamin P. Flower, and Lawrence Krissek, (2004), Evolution Of Iceberg Melting, Biological Productivity, And The Record Of Icelandic Volcanism In The Irminger Basin Since 630 Ka, *Marine Geology* 212,1-4, 133-152.

Appendix

Contents:

Appendix A -

Grain Abundances	II–VI
------------------------	-------

Appendix B -

Total Terrestrial Grains vs. Age	VII
Total Biological Grains vs. Age	VIII
Total Other Grains vs. Age	IX
Total Coarse Grained Mafic Grains vs. Age	X
Total Quartz Grains vs. Age	XI
Total Fine Grained Mafic Grains vs. Age	XII
Total Volcanic Grains vs. Age	XIII
Total Sedimentary and Carbonate Fragments vs. Age	XIV

Appendix A

Table 3: Grain Distribution Down Core

Sample number	Depth (mcd)	Age for sample	% mudballs	% Forams/ Bio	% Quartz	% Coarse Grained Mafic	% Fine grained mafic	% Volcanic	% Iron Stained Quartz	% Rose quartz	% Pyritic	% Sed/ Carb. Fragments	% Terr	% Bio	% Mudballs
303-1308-C6-H5-(56-58)-60003147	55.58	851.5	42.6	30.6	4.6	12.0	3.7	0.9	1.9	0	0	3.7	26.9	30.6	42.6
303-1308-C6-H5-(56-58)-60003147 *	55.58	851.5	45.0	32.4	11.7	4.5	0	4.5	0	0	0	1.8	22.5	32.4	45.0
303-1308-C6-H5-(78-80)-60003148	55.8	854.25	43.3	1.9	9.6	9.6	4.8	13.5	1.0	0	0	16.3	54.8	1.9	43.3
303-1308-C6-H5-(106-108)-60003149	56.08	857.75	18.4	37.9	18.4	6.8	1.9	0	2.9	0	0	13.6	43.7	37.9	18.4
303-1308-C6-H5-(106-108)-60003149*	56.08	857.75	16.4	58.2	7.3	11.8	0.9	0	0.9	0	0	4.5	25.5	58.2	16.4
303-1308-C6-H5-(128-130)-60003150	56.3	860.5	9.3	55.1	1.9	10.3	1.9	0	0.9	0	0	20.6	35.5	55.1	9.3
303-1308-F6-H3-(6-8)-80002761*	56.43	862.125	N/A	N/A	N/A	N/A	N/A	N/A	N/A	N/A	N/A	N/A	N/A	N/A	N/A
303-1308-F6-W3-(28-30)-80002762	56.65	864.875	0	0	4.9	16.7	6.9	2.0	0	0	0	69.6	100	0	0

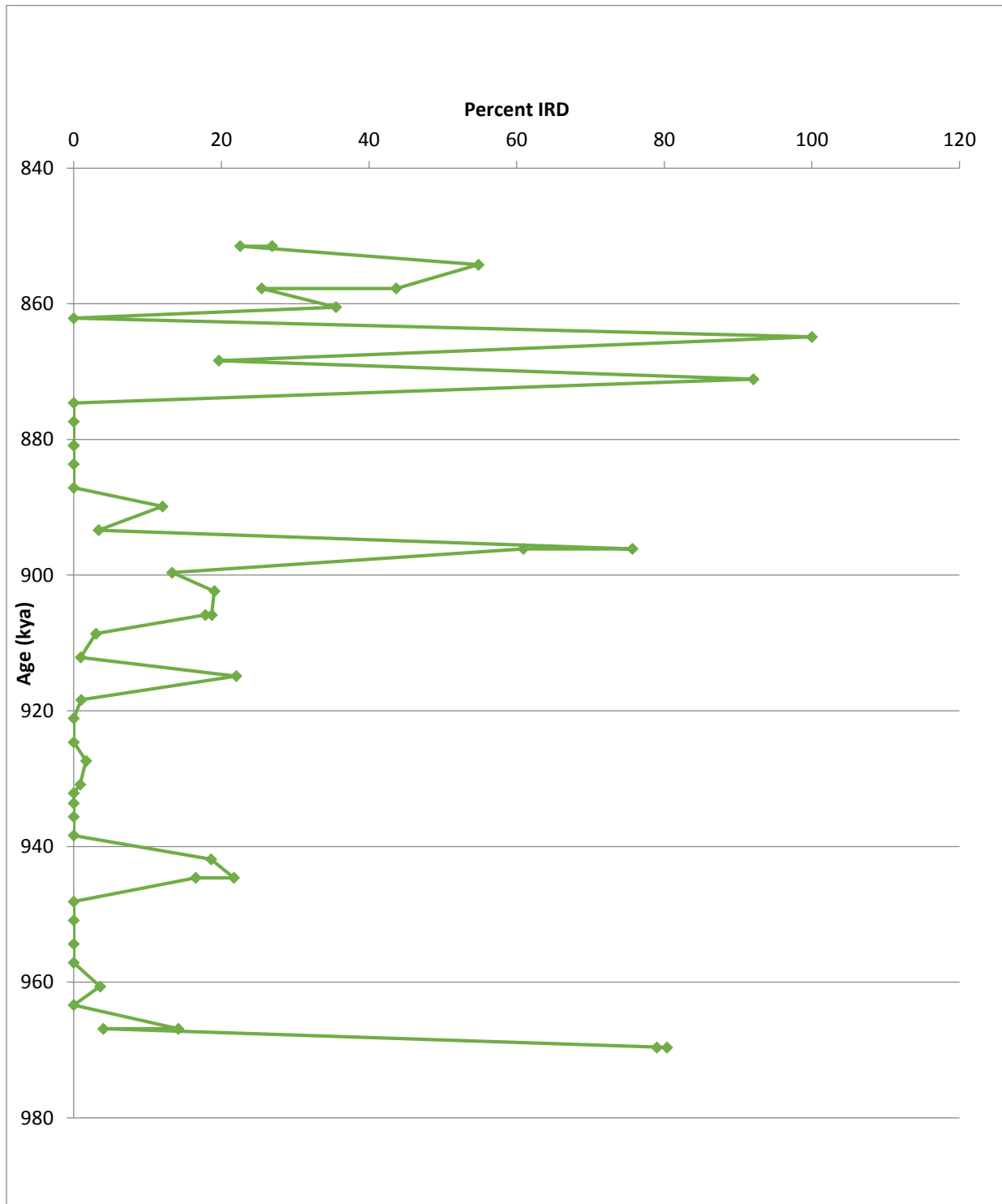
Sample number	Depth (mcd)	age for sample	% mud balls	% Forams/ Bio	% Quartz	% Coarse Grained Mafic	% Fine grained mafic	% Volcanic	% Iron Stained Quartz	% Rose quartz	% Pyritic	% Sed/ Carb. Fragments	% Terr	% Bio	% Mudballs
303-1308-F6-W3-(56-58)-80002763	56.93	868.375	78.6	1.8	3.6	8.9	0.9	2.7	0	0	0	3.6	19.6	1.8	78.6
303-1308-F6-W3-(78-80)-80002764	57.15	871.125	7.9	0	3.0	12.9	24.8	0	0	0	0	51.5	92.1	0	7.9
303-1308-F6-W3-(106-108)-80002765	57.43	874.625	47.2	52.8	0	0	0	0	0	0	0	0	0	52.8	47.2
303-1308-F6-W3-(128-130)-80002766	57.65	877.375	60.8	39.2	0	0	0	0	0	0	0	0	0	39.2	60.8
303-1308-F6-H4-(6-8)-80002925	57.93	880.875	20.4	72.4	0	0	0	0	0	0	7.1	0	0	72.4	20.4
303-1308-F6-H4-(6-8)-80002925*	57.93	880.875	24	75	0	0	0	0	0	0	1	0	0	75	24
303-1308-F6-H4-(28-30)-80002926	58.15	883.625	22.1	75.2	0	0	0	0	0	0	2.7	0	0	75.2	22.1
303-1308-F6-W4-(56-58)-80002927	58.43	887.125	86.6	13.4	0	0	0	0	0	0	0	0	0	13.4	86.6
303-1308-F6-W4-(78-80)-80002928	58.65	889.875	79	9	0	0	0	0	0	0	0	12	12	9	79
303-1308-F6-H4-(106-108)-80002929	58.93	893.375	65.5	31.1	0	0.8	2.5	0	0	0	0	0	3.4	31.1	65.5

Sample number	Depth (mcd)	age for sample	% mud balls	% Forams/ Bio	% Quartz	% Coarse Grained Mafic	% Fine grained mafic	% Volcanic	% Iron Stained Quartz	% Rose quartz	% Pyritic	% Sed/ Carb. Fragments	% Terr	% Bio	% Mudballs
303-1308-F6-H4-(128-130)-80002930	59.15	896.125	15.0	9.3	8.4	11.2	15.0	9.3	1.9	0	0	29.9	75.7	9.3	15.0
303-1308-F6-H4-(128-130)-80002930*	59.15	896.125	21.8	17.3	6.4	9.1	7.3	10.9	0.9	0	0	26.4	60.9	17.3	21.8
303-1308-F6-W5-(6-8)-80003089	59.43	899.625	32.4	54.3	0	5.7	0	1.0	0	0	0	6.7	13.3	54.3	32.4
303-1308-F6-H5-(28-30)-80003090	59.65	902.375	44.8	36.2	1.0	1.9	2.9	2.0	0	0	0	11.4	19.0	36.2	44.8
303-1308-F6-H5-(56-58)-80003091	59.93	905.875	64.5	16.8	3.7	5.6	1.9	4.7	0	0	0	2.8	18.7	16.8	64.5
303-1308-F6-H5-(56-58)-80003091*	59.93	905.875	66.3	15.8	4.0	2.0	0	11.9	0	0	0	0	17.8	15.8	66.3
303-1308-F6-W5-(78-80)-80003092	60.15	908.625	93	4	1	1	0	0	0	0	0	1	3	4	93
303-1308-F6-W5-(106-108)-80003093	60.43	912.125	69.2	29.9	0	0	0	0	0	0	0	0.9	0.9	29.9	69.2
303-1308-F6-W5-(128-130)-80003094	60.65	914.875	9	69	1	2	3	0	0	0	0	16	22	69	9
303-1308-F6-H6-(6-8)-80003245	60.93	918.375	11.9	86.1	1.0	0	0	0	0	0	1.0	0	1.0	86.1	11.9
303-1308-F6-W6-(28-30)-80003246	61.15	921.125	82.5	17.5	0	0	0	0	0	0	0	0	0	17.5	82.5

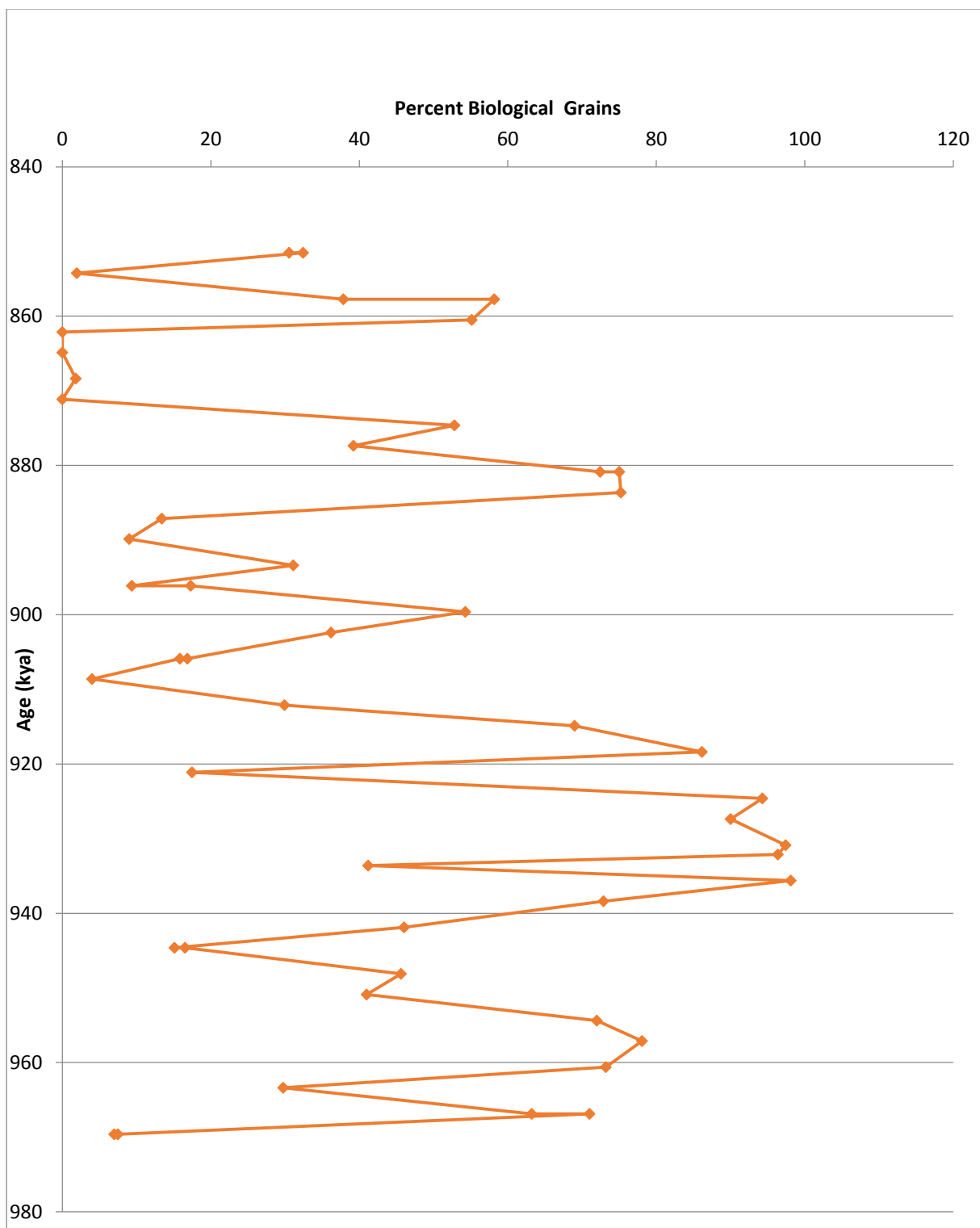
Sample number	Depth (mcd)	age for sample	% mud balls	% Forams/ Bio	% Quartz	% Coarse Grained Mafic	% Fine grained mafic	% Volcanic	% Iron Stained Quartz	% Rose quartz	% Pyritic	% Sed/ Carb. Fragments	% Terr	% Bio	% Mudballs
303-1308-F6-W6-(56-58)-80003247	61.43	924.625	5.7	94.3	0	0	0	0	0	0	0	0	0	94.3	5.7
303-1308-F6-H6-(78-80)-80003248	61.65	927.375	7.5	90	0	0	0	0	0	0	0.8	1.7	1.7	90	7.5
303-1308-F6-H6-(106-108)-80003249	61.93	930.875	1.7	97.4	0	0	0	0	0	0	0	0.9	0.9	97.4	1.7
303-1308-B7-H3-(28-30)-50000996	62.03	932.125	2.7	96.4	0	0	0	0	0	0	0.9	0	0	96.4	2.7
303-1308-F6-W6-(128-130)-80003250	62.15	933.625	58.8	41.2	0	0	0	0	0	0	0	0	0	41.2	58.8
303-1308-B7-H3-(56-58)-50000997	62.31	935.625	1.9	98.1	0	0	0	0	0	0	0	0	0	98.1	1.9
303-1308-B7-H3-(78-80)-50000998	62.53	938.375	27.1	72.9	0	0	0	0	0	0	0	0	0	72.9	27.1
303-1308-B7-H3-(106-108)-50000999	62.81	941.875	35.4	46.0	4.4	8.8	1.8	0	0	0	0	3.5	18.9	46.0	35.4
303-1308-B7-H3-(128-130)-50001000	63.03	944.625	63.2	15.1	1.9	9.4	0	0.9	0	0	0	9.4	21.7	15.1	63.2
303-1308-B7-H3-(128-130)-50001000*	63.03	944.625	67.0	16.5	1.9	6.8	1.0	2.9	0	0	0	3.9	16.5	16.5	67.0
303-1308-B7-H4-(6-8)-50001139	63.31	948.125	53.5	45.6	0	0	0	0	0	0	0.9	0	0	45.6	53.5

Sample number	Depth (mcd)	age for sample	% mud balls	% Forams/ Bio	% Quartz	% Coarse Grained Mafic	% Fine grained mafic	% Volcanic	% Iron Stained Quartz	% Rose quartz	% Pyritic	% Sed/ Carb. Fragments	% Terr	% Bio	% Mudballs
303-1308-B7-H4-(28-30)-50001140	63.53	950.875	58	41	0	0	0	0	0	0	1	0	0	41	58
303-1308-B7-H4-(56-58)-50001141	63.81	954.375	26	72	0	0	0	0	0	0	2	0	0	72	26
303-1308-B7-H4-(78-80)-50001142	64.03	957.125	20	78.1	0	0	0	0	0	0	1.9	0	0	78.1	20
303-1308-B7-H4-(106-108)-50001143	64.31	960.625	15.2	73.2	1.8	1.8	0	0	0	0	8.0	0	3.6	73.2	15.2
303-1308-B7-H4-(128-130)-50001144	64.53	963.375	70.3	29.7	0	0	0	0	0	0	0	0	0	29.7	70.3
303-1308-B7-H5-(6-8)-50001288	64.81	966.875	22.6	63.2	5.7	1.9	2.8	0	0	0.9	0	2.8	14.2	63.2	22.6
303-1308-B7-H5-(6-8)-50001288*	64.81	966.875	25	71	3	0	0	0	0	0	0	1	4	71	25
303-1308-B7-H5-(28-30)-50001289	65.03	969.625	12.1	7.5	16.8	8.4	20.6	5.6	0	1.9	0	27.1	80.4	7.5	12.1
303-1308-B7-H5-(28-30)-50001289*	65.03	969.625	14	7	9	18	10	11	0	0	0	31	79	7	14

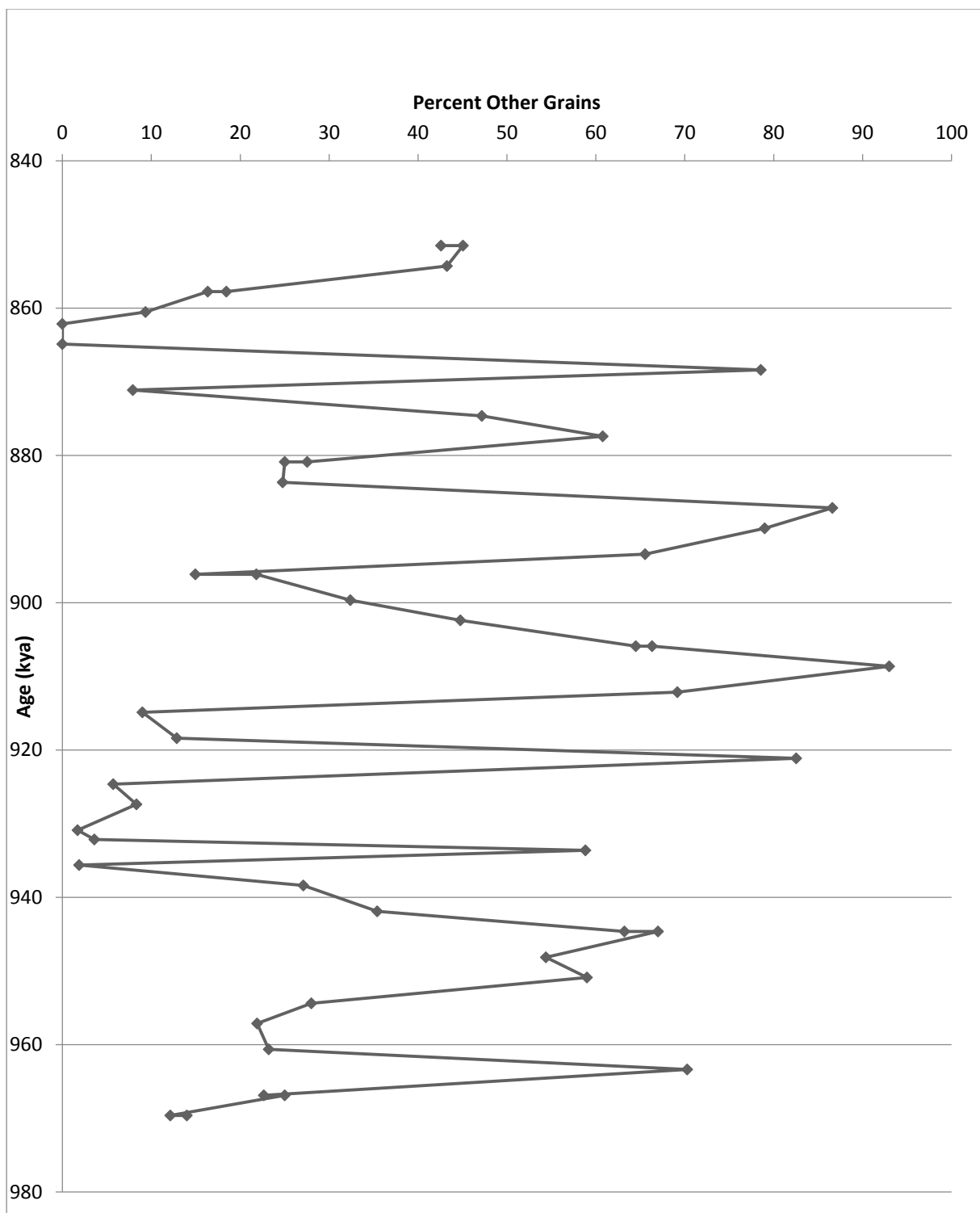
Appendix B



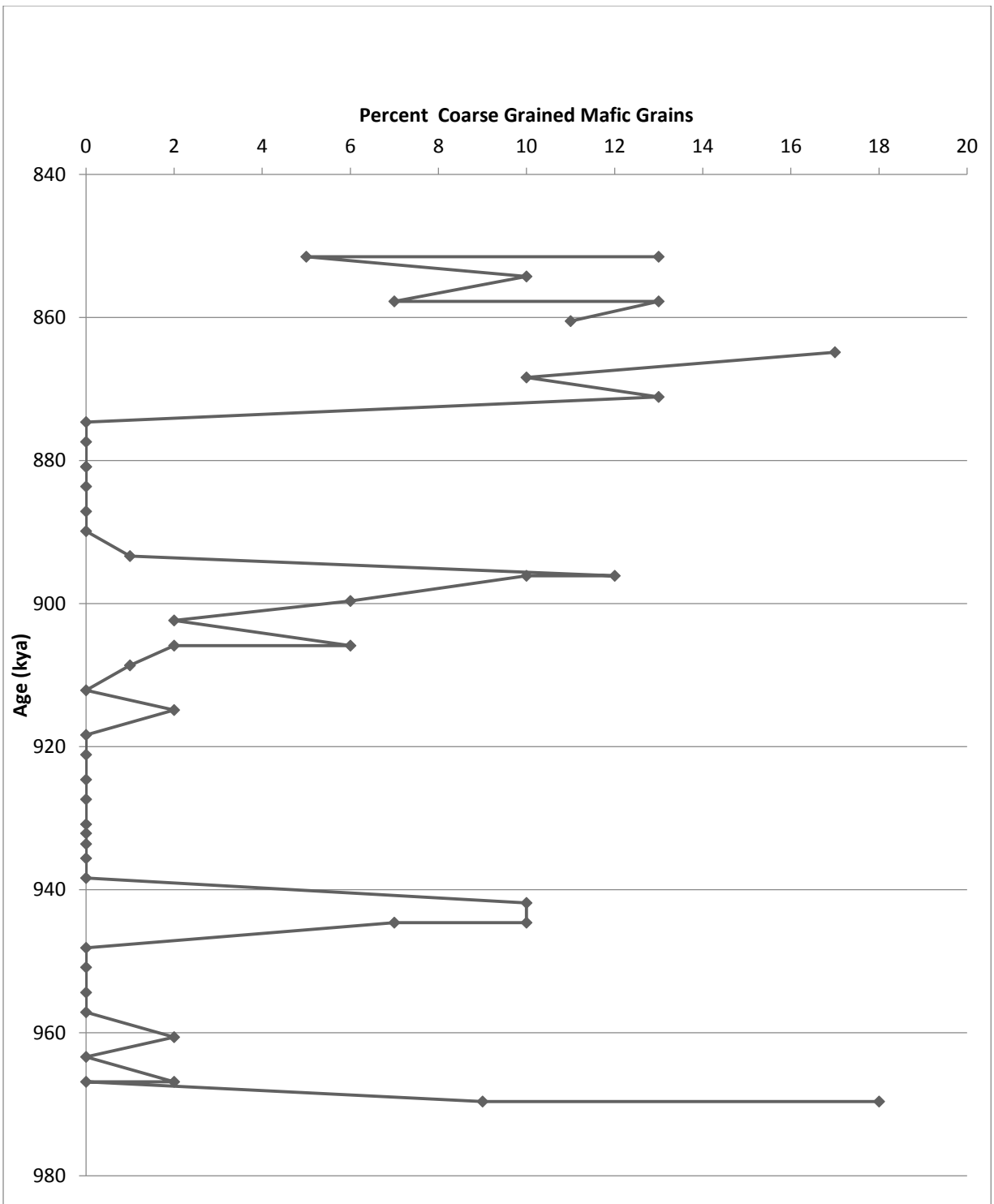
Total abundance of terrestrial grains in sample in relation to age in thousands of years.



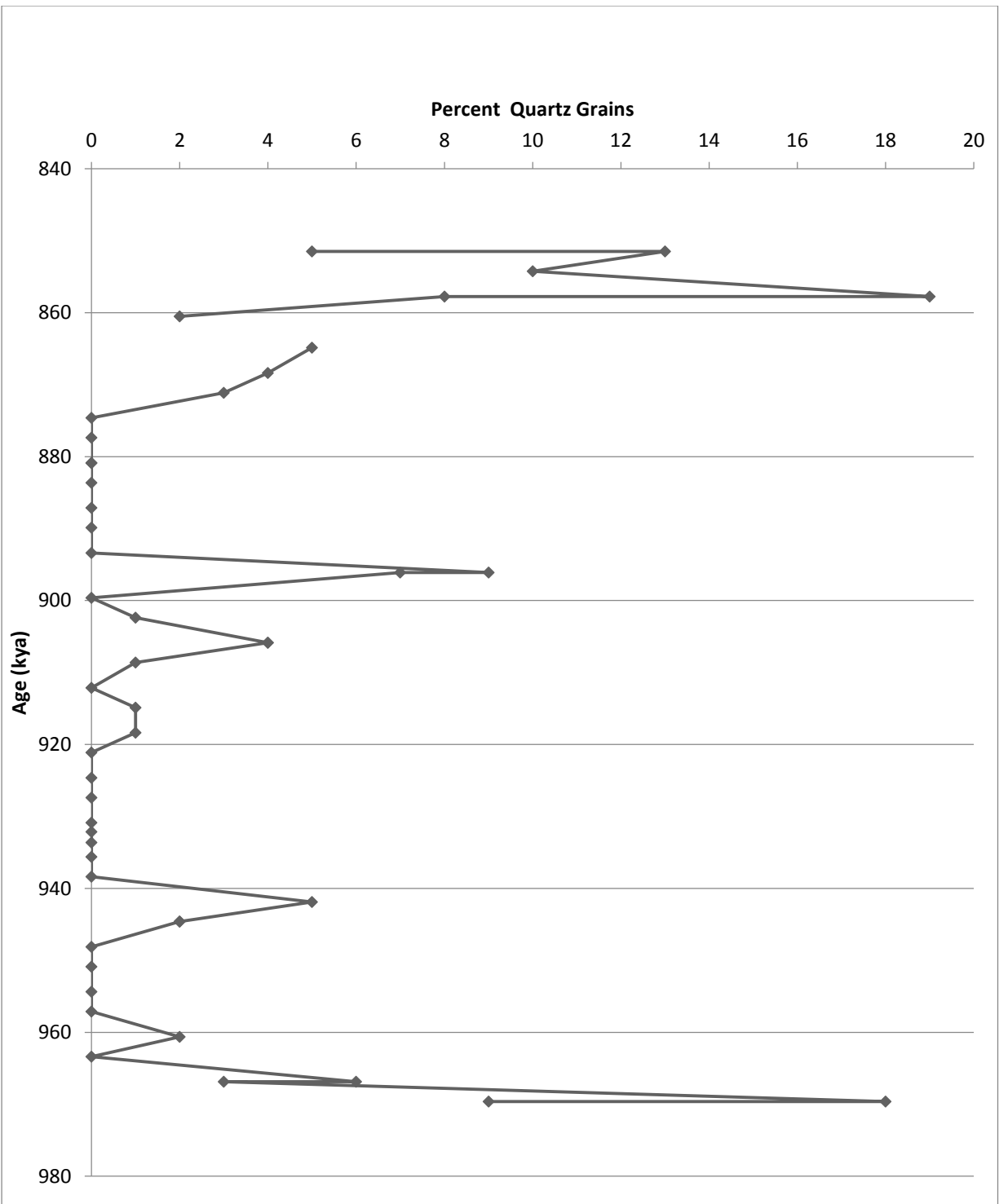
Total abundance of biological grains in sample in relation to age in thousands of years.



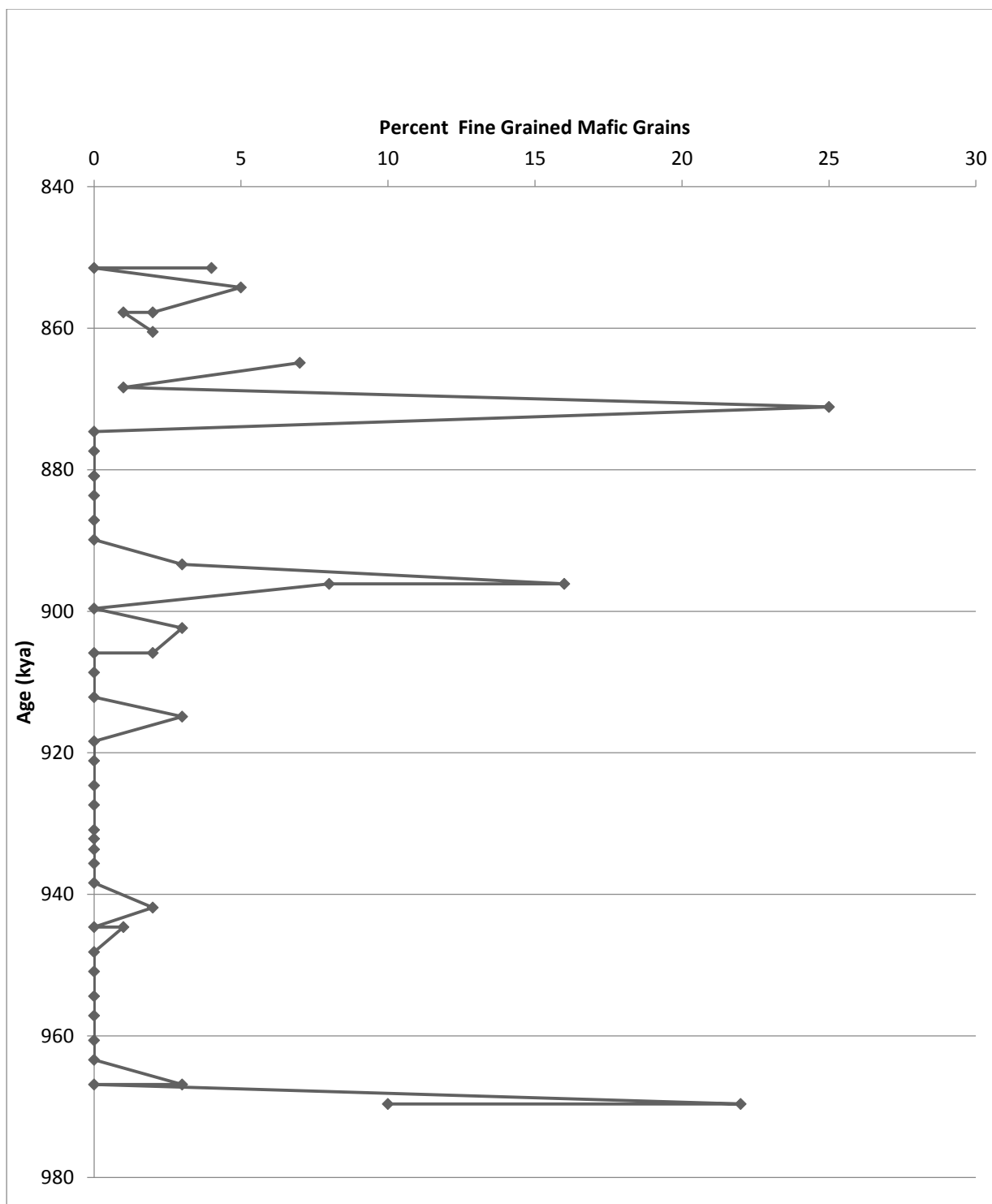
Total abundance of other grains in sample in relation to age in thousands of years.



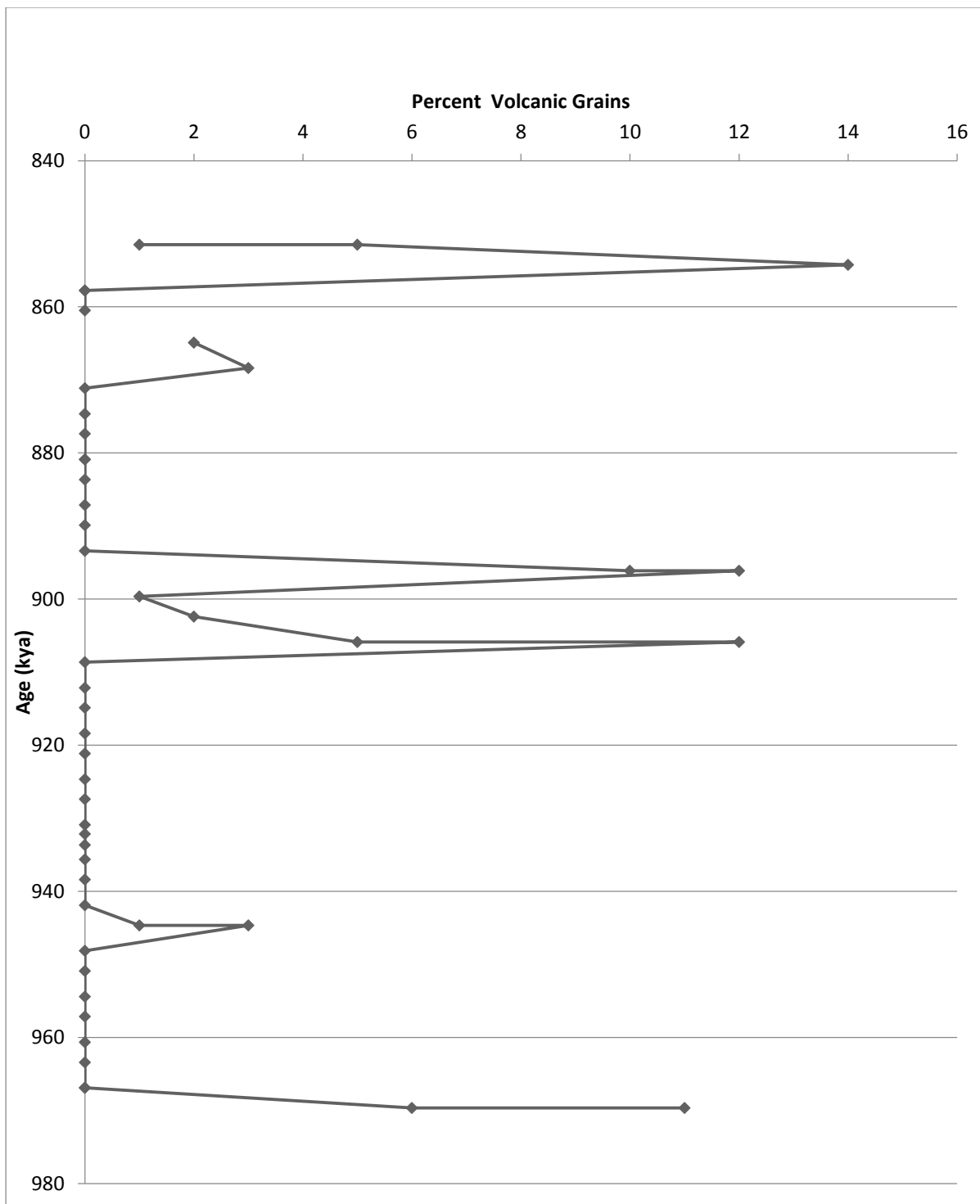
Total abundance of coarse grained mafic grains in sample in relation to age in thousands of years.



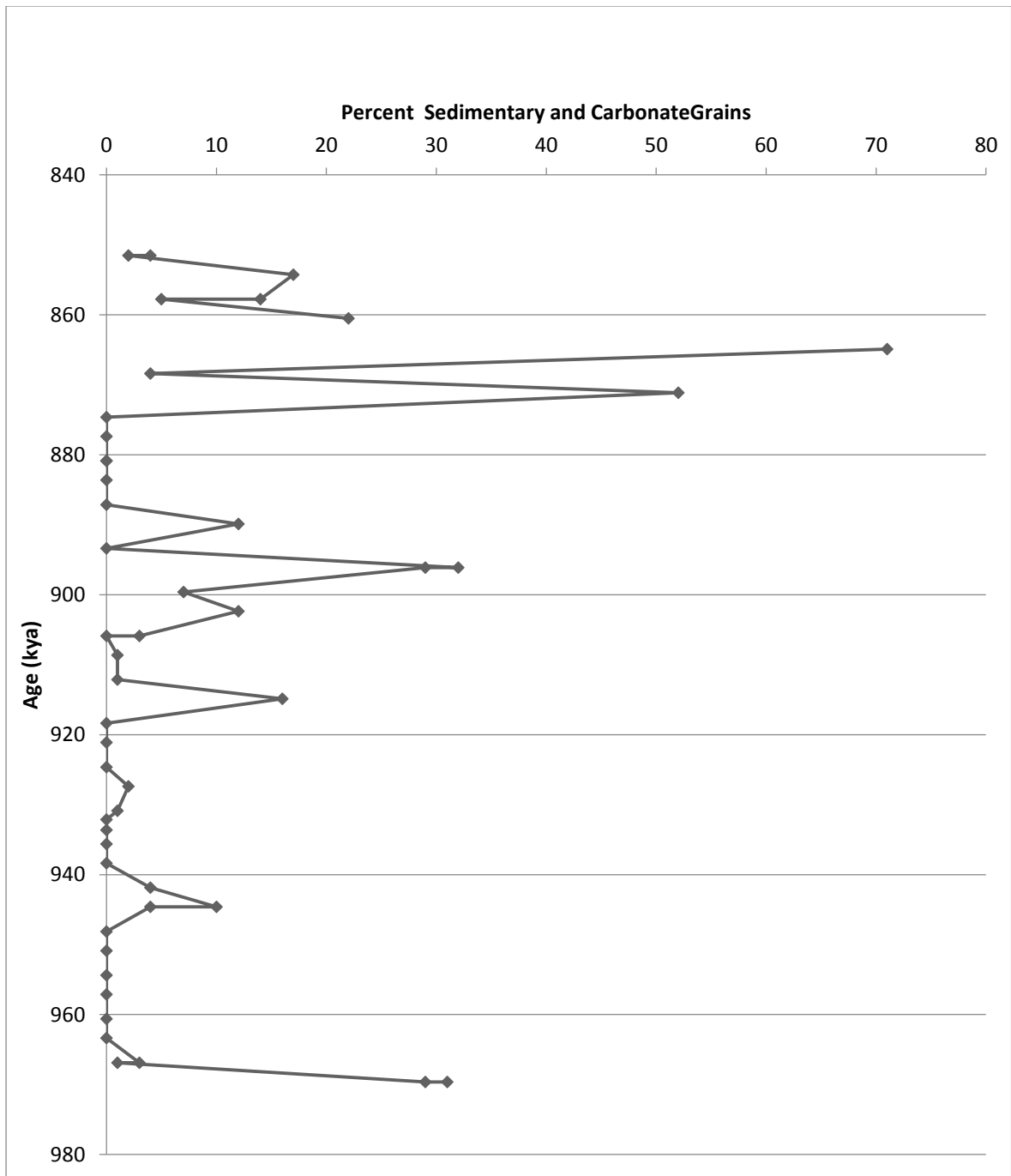
Total abundance of quartz grains in sample in relation to age in thousands of years.



Total abundance of fine grained mafic grains in sample in relation to age in thousands of years.



Total abundance of volcanic grains in sample in relation to age in thousands of years.



Total abundance of sedimentary and carbonate fragment grains in sample in relation to age in thousands of years.